

## **SUPPLEMENTARY INFORMATION**

### **Spatiotemporal resolution of the Ntla transcriptome in axial mesoderm development**

Ilya A. Shestopalov<sup>1</sup>, Cameron L. W. Pitt<sup>1</sup>, and James K. Chen<sup>1</sup>

<sup>1</sup>Department of Chemical and Systems Biology, Stanford University School of Medicine,  
Stanford, CA 94305, USA

## SUPPLEMENTARY RESULTS

<b>Supplementary Table 1</b> .....	3-6
<b>Supplementary Table 2</b> .....	7
<b>Supplementary Table 3</b> .....	8-9
<b>Supplementary Table 4</b> .....	10-11
<b>Supplementary Table 5</b> .....	12
<b>Supplementary Table 6</b> .....	13-15
<b>Supplementary Table 7</b> .....	16
<b>Supplementary Table 8</b> .....	17-18
<b>Supplementary Table 9</b> .....	19
<b>Supplementary Table 10</b> .....	20
<b>Supplementary Table 11</b> .....	21-24
<b>Supplementary Table 12</b> .....	25
<b>Supplementary Table 13</b> .....	26
<b>Supplementary Figure 1</b> .....	27
<b>Supplementary Figure 2</b> .....	28
<b>Supplementary Figure 3</b> .....	29
<b>Supplementary Figure 4</b> .....	30
<b>Supplementary Figure 5</b> .....	31
<b>Supplementary Figure 6</b> .....	32
<b>Supplementary Figure 7</b> .....	33
<b>Supplementary Figure 8</b> .....	34
<b>Supplementary Figure 9</b> .....	35

**Supplementary Table 1. cFD vs. *ntl*a cMO + cFD comparison at 9 hpf: 87 microarray hits ranked by fold change.**

Ensembl ID and chromosome locations correspond to zebrafish genome assembly Zv8, gene build 59 (May 2010).

Entry	Gene symbol	Gene description	Fold change	Zfin ID	Ensembl gene ID	Nimblegen SEQ_ID	Chr	Start	End
1	<i>si:ch211-215a10.5-001 (hpcal4)</i>	novel protein similar to vertebrate hippocalcin like 4	-6.543	<i>si:ch211-215a10.5-001</i>	<i>NP_001108159.1</i>	OTTDART00000018441	19	29460115	29462786
2	<i>LOC563543 (inpp5b)</i>	novel protein similar to vertebrate inositol polyphosphate-5-phosphatase	-6.093	none	<i>LOC563543</i>	ZV700S00001662	16	2599817	2639066
3	<i>lhx1a</i>	LIM-homeobox 1a	-6.092	<i>lhx1a</i>	<i>lhx1a</i>	AW077429	15	28135534	28143145
4	<i>snai2</i>	snail homolog 2	-5.700	<i>snai2</i>	<i>snai2</i>	OTTDART00000027124	24	33995692	34001705
5	<i>notch1b</i>	notch homolog 1b	-5.524	<i>notch1b</i>	<i>notch1b</i>	OTTDART00000023258	5	67392870	67496053
6	<i>si:dkey-49o11.4 (tbx3l)</i>	novel protein similar to vertebrate t-box 3	-5.072	<i>si:dkey-49o11.4</i>	<i>LOC568479</i>	OTTDART00000019838	5	24885216	24887665
7	<i>wnt8a</i>	wingless-type MMTV integration site family, member 8a	-4.652	<i>wnt8a</i>	<i>wnt8a</i>	OTTDART00000025914	14	36040558	36047793
8	<i>LOC566628 (pskh2)</i>	novel protein similar to vertebrate protein serine kinase H2	-4.616	none	<i>LOC566628</i>	ENSDART00000037703	12	40283700	40307825
9	<i>lrrc8da</i>	novel protein similar to vertebrate leucine rich repeat containing 8 family, member D alpha	-4.602	<i>lrrc8da</i>	<i>A2BIH6_DANRE</i>	OTTDART00000023505	2	22633903	22636380
10	<i>atp1a1b</i>	ATPase, Na+/K+ transporting, alpha 1b polypeptide	-4.371	<i>atp1a1b</i>	<i>atp1a1b</i>	OTTDART00000026276	9	36416946	36437549
11	<i>myod1</i>	myogenic determination factor 1	-4.290	<i>myod1</i>	<i>myod1</i>	OTTDART00000026919	25	32781654	32783858
12	<i>si:dkey-146l2.1-001 (ankrd15)</i>	novel protein similar to vertebrate ankyrin repeat domain 15	-4.281	<i>si:dkey-146l2.1-001</i>	<i>A2CEC3_DANRE</i>	TC243640	5	43852500	43944459
13	<i>zgc:91787 (b3gnt7)</i>	novel protein similar to vertebrate beta-3-galactosyltransferase	-4.215	<i>zgc:91787</i>	<i>zgc:91787</i>	OTTDART00000020258	8	22683762	22685318
14	<i>col8a1a</i>	collagen, type VIII, alpha 1	-4.113	<i>col8a1a</i>	<i>col8a1a</i>	AI397462	9	30487274	30499313
15	<i>plp2</i>	proteolipid protein 2	-4.036	<i>plp2</i>	<i>plp2</i>	TC260151	8	50452420	50499168
16	<i>plod1a</i>	lysyl hydroxylase 1	-3.848	<i>plod1a</i>	<i>plod1a</i>	ZV700S00006183	8	49269611	49320332
17	<i>ribc1</i>	RIB43A domain with coiled-coils 1	-3.614	<i>ribc1</i>	<i>zgc:158280</i>	ZV700S00001481	23	28138233	28145545
18	<i>pip5k1c</i>	phosphatidylinositol-4-phosphate 5-kinase, type I, gamma	-3.592	<i>pip5k1c</i>	<i>pip5k1c</i>	ENSDART00000105443	22	17671179	17691603
19	<i>pde4ba</i>	cAMP-specific 3',5'-cyclic phosphodiesterase 4B alpha	-3.547	<i>pde4ba</i>	<i>LOC565706</i>	ZV700S00006639	6	32670067	32747756
20	<i>rbm38</i>	RNA binding motif protein 38	-3.483	<i>rbm38</i>	<i>rbm38</i>	OTTDART00000026624	23	4620570	4666179
21	<i>lamp1</i>	lysosomal-associated membrane protein 1	-3.426	<i>lamp1</i>	none	ZV700S00006436	9	34697159	34701323
22	<i>cpn1</i>	carboxypeptidase N, polypeptide 1	-3.379	<i>cpn1</i>	<i>cpn1</i>	BC066689.1	12	30496591	30523965
23	<i>abcc6b</i>	ATP-binding cassette, sub-family C, member 6b	-3.344	<i>abcc6b</i>	<i>abcc6</i>	ENSDART00000065433	6	11984572	12024328
24	<i>dopey2</i>	dopey family member 2	-3.341	<i>dopey2</i>	<i>dopey2</i>	ENSDART00000078256	9	33581620	33595018

25	<i>kirrel3l</i>	kin of IRRE like 3 like	-3.334	<i>kirrel3l</i>	<i>kirrel3l</i>	ZV700S00005154	9	26637783	26712362
26	<i>aldh1a2</i>	aldehyde dehydrogenase 1 family, member A2	-3.255	<i>aldh1a2</i>	<i>aldh1a2</i>	OTTDART00000025116	7	30625839	30666282
27	<i>mxn1</i>	motor neuron and pancreas homeobox 1	-3.252	<i>mxn1</i>	<i>mxn1</i>	OTTDART00000013585	7	41141692	41144486
28	<i>caskin1</i>	CASK-interacting protein 1	-3.206	none	<i>ENSDARG00000046107</i>	ENSDART00000040925	3	32954587	32996156
29	<i>hmbox1b</i>	similar to homeobox containing 1	-3.133	<i>hmbox1b</i>	<i>LOC564816</i>	ENSDART00000008808	Zv8_NA11417	178371	190934
30	<i>pak1</i>	P21/Cdc42/Rac1-activated kinase 1	-3.114	<i>pak1</i>	<i>pak1</i>	ZV700S00006164	18	2188979	2204559
31	<i>ppargc1a1</i>	peroxisome proliferator activated receptor gamma coactivator 1 alpha - like	-3.026	<i>ppargc1a1</i>	<i>ppargc1a1</i>	ENSDART00000077731	Zv8_NA6114	4577	28421
32	<i>unc45b</i>	homolog of <i>C. elegans</i> unc-45B	-3.013	<i>unc45b</i>	<i>unc45b</i>	OTTDART00000024993	8	10979015	11004475
33	<i>zgc:66052 (tagln3b)</i>	novel protein similar to vertebrate transgelin 3	-2.939	<i>zgc:66052</i>	<i>zgc:66052</i>	OTTDART00000028979	24	21471592	21485670
34	<i>tbx6</i>	T-box gene 6	-2.919	<i>tbx6</i>	<i>tbx6</i>	OTTDART00000022473	5	41292606	41309337
35	<i>myf5</i>	myogenic factor 5	-2.788	<i>myf5</i>	<i>myf5</i>	OTTDART00000009544	4	21534374	21538246
36	<i>hdr</i>	hematopoietic death receptor	-2.773	<i>hdr</i>	<i>hdr</i>	OTTDART00000019823	5	25528873	25539033
37	<i>rgmb</i>	RGM domain family, member B	-2.721	<i>rgmb</i>	<i>rgmb</i>	OTTDART00000022855	5	48756554	48774922
38	<i>trpv4</i>	transient receptor potential cation channel, subfamily V, member 4	-2.712	<i>trpv4</i>	<i>trpv4</i>	OTTDART00000019252	5	17734760	17772071
39	<i>tacc2</i>	transforming, acidic coiled-coil containing protein 2	-2.693	<i>tacc2</i>	<i>tacc2</i>	ZV700S00006103	13	33046650	33082675
40	<i>adora2ab</i>	adenosine receptor A2a.2	-2.677	<i>adora2ab</i>	<i>NP_001035125.1</i>	NM_001040036	21	10544202	10563719
41	<i>hspa12a</i>	heat shock 70 kDa protein 12A	-2.660	<i>hspa12a</i>	<i>zgc:153612</i>	ZV700S00001957	17	18786426	18805408
42	<i>zgc:153027 (esm1)</i>	novel protein similar to vertebrate endothelial cell-specific molecule 1	-2.637	<i>zgc:153027</i>	<i>zgc:153027</i>	TC263451	21	8194010	8198200
43	<i>kidins220a</i>	kinase D-interacting substance of 220 kDa	-2.603	<i>kidins220a</i>	<i>si:dkey-177f17.1</i>	OTTDART00000007862	17	33031518	33087170
44	<i>si:dkey-195c14.1 (sall3l)</i>	novel protein similar to vertebrate sal-like 3	-2.552	<i>si:dkey-195c14.1</i>	<i>si:dkey-195c14.1</i>	OTTDART00000017492	19	20764504	20773732
45	<i>smyd1b</i>	SET and MYND domain containing 1b	-2.532	<i>smyd1b</i>	<i>smyd1b</i>	NM_001039636	8	1232945	1278872
46	<i>her1</i>	hairy-related 1	-2.529	<i>her1</i>	<i>her1</i>	OTTDART00000023081	5	70458828	70465219
47	<i>p4ha1</i>	procollagen-proline, 2-oxoglutarate 4-dioxygenase (proline 4-hydroxylase), alpha polypeptide I	-2.512	<i>p4ha1</i>	<i>p4ha1</i>	OTTDART00000025381	17	16492035	16511758
48	<i>hfe2</i>	hemochromatosis type 2	-2.485	<i>hfe2</i>	<i>hfe2</i>	NM_213643	16	42382086	42527246
49	<i>zgc:163023 (tspan4)</i>	novel protein similar to vertebrate tetraspanin 4	-2.460	<i>zgc:163023</i>	<i>zgc:163023</i>	NM_001082807	3	29844005	29853390
50	<i>lrch2</i>	leucine-rich repeats and calponin homology (CH) domain containing 2	-2.431	<i>lrch2</i>	<i>lrch2</i>	OTTDART00000030270	5	34818824	34844320
51	<i>lipg</i>	lipase, endothelial	-2.429	<i>lipg</i>	<i>lipg</i>	OTTDART00000028618	8	33133042	33142110
52	<i>ttna</i>	titin a	-2.415	<i>ttna</i>	<i>ttna</i>	OTTDART00000029928	9	43263480	43328198
53	<i>itgb5</i>	integrin, beta 5	-2.400	<i>itgb5</i>	<i>itgb5</i>	OTTDART00000014003	9	22031250	22101761
54	<i>actn2</i>	actinin, alpha 2	-2.384	<i>actn2</i>	<i>actn2</i>	OTTDART00000029626	17	16515238	16537141
55	<i>zgc:92198 (camk2n2)</i>	novel protein similar to vertebrate Ca <sup>2+</sup> /calmodulin-dependent protein kinase II inhibitor 2	-2.367	<i>zgc:92198</i>	<i>zgc:92198</i>	NM_001002642	24	25360048	25362300

56	<i>fadd</i>	fas (tnfrsf6)-associated via death domain	-2.341	<i>fadd</i>	<i>fadd</i>	TC242683	7	55882294	55888612
57	<i>wnt3l</i>	wingless-type MMTV integration site family, member 3 like	-2.338	<i>wnt3l</i>	<i>wnt3l</i>	NM_001007185	2	2309950	2311326
58	<i>mesp2</i>	mesoderm posterior 2 homolog	-2.333	<i>mesp2</i>	<i>A3KPB3_DANRE</i>	ENSDART00000102928	25	9383009	9384267
59	<i>twist2</i>	twist 2	-2.333	<i>twist2</i>	<i>twist2</i>	NM_001005956	9	46391351	46391842
60	<i>ttnb</i>	titin b	-2.327	<i>ttnb</i>	<i>ttnb</i>	OTTDART00000026898	9	42989675	43130539
61	<i>st3gal2l</i>	ST3 beta-galactoside alpha-2,3-sialyltransferase 2, like	-2.321	<i>st3gal2l</i>	<i>st3gal2l</i>	TC249907	11	26392769	26414674
62	<i>sort1b</i>	sortilin 1, like	-2.284	<i>sort1b</i>	<i>sort1b</i>	OTTDART00000013761	8	25809473	25842079
63	<i>hmcn1</i>	hemicentin 1	-2.272	<i>hmcn1</i>	<i>hmcn1</i>	OTTDART00000006813	20	34056841	34169854
64	<i>irx3a</i>	iroquois homeobox protein 3a	-2.242	<i>irx3a</i>	<i>irx3a</i>	ZV700S00006366	7	36391615	36394934
65	<i>sall1a</i>	sal-like 1a	-2.206	<i>sall1a</i>	<i>sall1a</i>	ZV700S00001341	7	37784931	37793542
66	<i>tnfaip6</i>	tumor necrosis factor, alpha-induced protein 6	-2.200	<i>tnfaip6</i>	<i>tnfaip6</i>	TC245382	9	22117982	22133555
67	<i>zgc:66433 (KIAA1211)</i>	novel protein similar to vertebrate uncharacterized protein KIAA1211	-2.200	<i>zgc:66433</i>	<i>zgc:66433</i>	OTTDART00000028901	14	22214800	22296654
68	<i>inka1a</i>	induced in neural crest by AP2, 1a	-2.170	<i>inka1a</i>	<i>inka1a</i>	ZV700S00000040	11	35101810	35108146
69	<i>meis4.1a</i>	myeloid ecotropic viral integration site 4.1a	-2.155	<i>meis4.1a</i>	<i>meis4.1a</i>	OTTDART00000023940	1	51288174	51319427
70	<i>dlc</i>	deltaC	-2.146	<i>dlc</i>	<i>dlc</i>	OTTDART00000025961	15	20634176	20639029
71	<i>kitlga</i>	kit ligand a	-2.145	<i>kitlga</i>	<i>kitlga</i>	ENSDART00000104502	25	18638925	18658676
72	<i>prickle2</i>	prickle-like 2	-2.135	<i>prickle2</i>	<i>prickle2</i>	AY278987.1	11	18849431	18895050
73	<i>wwp2</i>	WW domain containing E3 ubiquitin protein ligase 2	-2.121	<i>wwp2</i>	<i>wwp2</i>	TC261671	25	34924572	34978790
74	<i>ENSDARG00000063075 (c20orf117)</i>	novel protein similar to vertebrate uncharacterized protein c20orf117	-2.120	none	<i>ENSDARG00000063075</i>	ENSDART00000091852	23	8047246	8130572
75	<i>ube2e3</i>	ubiquitin-conjugating enzyme E2E 3	-2.120	<i>ube2e3</i>	<i>ube2e3</i>	OTTDART00000026433	9	44146061	44228245
76	<i>kif1b</i>	kinesin family member 1B	-2.085	<i>kif1b</i>	<i>kif1b</i>	ZV700S00001465	23	28894800	28957280
77	<i>notch2</i>	notch homolog 2	-2.072	<i>notch2</i>	<i>notch2</i>	ZV700S00005786	8	19943482	19983080
78	<i>si:ch211-285f17.1 (KIAA1217)</i>	novel protein similar to vertebrate sickle tail protein homolog	-2.030	<i>si:ch211-285f17.1</i>	<i>ENSDARG00000031658</i>	TC253143	24	9246424	9333914
79	<i>id:ibd2573 (creb3l1)</i>	novel protein similar to vertebrate cAMP responsive element binding protein 3-like 1	-2.021	<i>id:ibd2573</i>	<i>LOC566720</i>	ENSDART00000074532	7	39330933	39358257
80	<i>fgf24</i>	fibroblast growth factor 24	-2.020	<i>fgf24</i>	<i>fgf24</i>	OTTDART0000002076	14	6156422	6194919
81	<i>tnfrsfa</i>	tumor necrosis factor receptor superfamily, member a	-2.013	<i>tnfrsfa</i>	<i>tnfrsfa</i>	ZV700S00000235	21	16565637	16612107
82	<i>zgc:165655</i>	novel pleckstrin domain protein	-2.009	<i>zgc:165655</i>	<i>zgc:165655</i>	NM_001098779	16	34734527	34792568
82/87 (94%) downregulated									
83	<i>myom3</i>	myomesin family, member 3	+2.002	<i>myom3</i>	<i>myom3</i>	ENSDART00000101501	Zv8_NA513	18129	78285
84	<i>nmnat2</i>	nicotinamide nucleotide adenyltransferase 2	+2.027	<i>nmnat2</i>	<i>nmnat2</i>	OTTDART00000020501	2	34068428	34082906
85	<i>hbp1</i>	HMG box-containing protein 1	+2.037	<i>hbp1</i>	<i>zgc:112297</i>	AW282104	25	2564423	2584269

86	<i>rbms3</i>	Single-stranded RNA interacting protein	+2.095	<i>rbms3</i>	<i>rbms3</i>	TC267504	16	38456043	38671893
87	<i>pdgfrb2</i>	platelet-derived growth factor receptor beta 1.2 fragment	+2.442	<i>pdgfrb2</i>	<i>pdgfrb2</i>	ENSDART00000028255	14	4208337	4211507
5/87 (6%) upregulated									

**Supplementary Table 2. cFD vs. *ntla* cMO + cFD comparison at 16 hpf: 12 microarray hits ranked by fold change.**

Ensembl ID and chromosome locations correspond to zebrafish genome assembly Zv8, gene build 59 (May 2010).

Entry	Gene symbol	Gene description	Fold change	Zfin ID	Ensembl gene ID	Nimblegen SEQ_ID	Chr	Start	End
1	<i>LOC795255 (slc38a8)</i>	novel protein similar to vertebrate soluble carrier family 38 protein	-4.917	none	<i>LOC795255</i>	BQ132767	7	29413983	29422236
2	<i>cav3</i>	caveolin 3	-2.717	<i>cav3</i>	<i>cav3</i>	AY124574.1	6	45637427	45645163
3	<i>znf385b</i>	zinc finger protein 385b	-2.357	<i>znf385b</i>	<i>znf385b</i>	OTTDART00000001965	9	43499966	43886239
4	<i>tspan7b</i>	tetraspanin 7b	-2.318	<i>tspan7b</i>	<i>tspan7b</i>	ZV700S00005092	22	13702361	13754893
5	<i>si:dkey-205o12.2 (prk1)</i>	novel protein similar to vertebrate pim oncogene related kinase 1	-2.073	<i>si:dkey-205o12.2</i>	<i>si:dkey-205o12.2</i>	ENSDART00000100940	8	13504646	13505939
6	<i>si:dkeyp-122e7.1 (znf804a)</i>	novel protein similar to vertebrate zinc finger 804a	-2.051	<i>si:dkeyp-122e7.1</i>	<i>ENSDARG00000027079</i>	ZV700S00000778	9	11484108	11611524
7	<i>ptrfb</i>	polymerase I and transcript release factor b	-2.046	<i>ptrfb</i>	<i>ptrfb</i>	ZV700S00003617	24	7593206	7623842
8	<i>zgc:174919</i>	novel protein containing zinc finger domain	-2.039	<i>zgc:174919</i>	<i>zgc:174919</i>	ENSDART00000106259	22	3102571	3109743
9	<i>zgc:110418 (kcnk6)</i>	novel protein similar to vertebrate potassium inwardly-rectifying channel, subfamily K, member 6	-2.030	<i>zgc:110418</i>	<i>zgc:110418</i>	TC241224	18	45049012	45058866
9/12 (75%) downregulated									
10	<i>wu:fd47f06 (guca2b)</i>	novel protein similar to vertebrate guanylate cyclase activator 2b	+2.095	<i>wu:fd47f06</i>	none	ENSDART0000028699	11	27970374	27971060
11	<i>ntla</i>	no tail-a	+2.225	<i>ntla</i>	<i>ntla</i>	ZV700S00001498	19	20033640	20038792
12	<i>frzb</i>	frizzled-related protein	+3.320	<i>frzb</i>	<i>frzb</i>	ZV700S00006289	9	47742998	47749719
3/12 (25%) upregulated									

**Supplementary Table 3. Microarray hits that overlap with previously reported Ntla targets.**

\*Mesodermal expression domains in gastrula-stage embryos (6-9 hpf)

\*\*Mesodermal expression domains in bud-stage embryos (10 hpf)

Entry	Gene symbol	Gene description	Expression domain in zebrafish	Previously reported direct target? <sup>1</sup>	Previously reported transcriptional target?
1	<i>dlc</i>	deltaC	Ventrolateral margin* Paraxial**	6 probes	No
2	<i>wnt8a</i>	wingless-type MMTV integration site family, member 8a	Ventrolateral margin* Tailbud**	5 probes, T-box clusters	Yes <sup>2</sup>
3	<i>aldh1a2</i>	aldehyde dehydrogenase 1 family, member A2	Ventrolateral margin* Paraxial**	4 probes, T-box clusters	1.5-fold decrease in expression upon loss of Ntla <sup>3</sup>
4	<i>her1</i>	hairy-related 1	Ventrolateral margin* Tailbud, Paraxial**	4 probes	1.5-fold decrease in expression upon loss of Ntla <sup>3</sup>
5	<i>kirrel3l</i>	kin of IRRE like 3 like	Axial, Margin* Axial**	3 probes, T-box clusters	No
6	<i>rbm38</i>	RNA binding motif protein 38	Tailbud, Paraxial**	3 probes	2.1-fold decrease in expression with loss of Ntla <sup>3</sup>
7	<i>irx3a</i>	iroquois homeobox protein 3a	Axial* Axial**	3 probes	No
8	<i>tbx6</i>	T-box gene 6	Ventrolateral margin* Tailbud, Paraxial**	2 probes, T-box clusters	1.7-fold decrease in expression with loss of Ntla <sup>3</sup>
9	<i>fgf24</i>	fibroblast growth factor 24	Margin* Tailbud, Paraxial**	2 probes, T-box clusters	No
10	<i>ube2e3</i>	ubiquitin-conjugating enzyme E2E 3	Not reported	2 probes	No
11	<i>myod1</i>	myogenic determination factor 1	Paraxial margin* Paraxial**	1 probe	No
12	<i>tnfaip6</i>	tumor necrosis factor, alpha-induced protein 6	Not reported	1 probe, T-box clusters	No
13	<i>zgc:66052 (tagln3b)</i>	novel protein similar to vertebrate transgelin 3	Axial, Other* Axial, Other**	T-box clusters	5.0-fold decrease in expression with loss of Ntla <sup>3</sup>
14	<i>zgc:163023 (tspan4)</i>	novel protein similar to vertebrate tetraspanin 4	Axial, Margin*	No	6.9-fold decrease in expression with loss of Ntla <sup>3</sup>
15	<i>hspa12a</i>	heat shock 70 kDa protein 12A	Not reported	No	4.4-fold decrease in expression with loss of Ntla <sup>3</sup>



16	<i>tacc2</i>	transforming, acidic coiled-coil containing protein 2	Axial, Margin* Axial**	No	2.7-fold decrease in expression with loss of Ntla <sup>3</sup>
17	<i>plp2</i>	proteolipid protein 2	Paraxial**	No	2.3-fold decrease in expression with loss of Ntla <sup>3</sup>

**Supplementary Table 4. cFD vs. *ntl*a cMO + cFD comparison at 9 hpf: 55 microarray hits with known expression patterns, grouped by their expression domain at 10 hpf and ranked by fold change.**

\*Expression domains highlighted in bold font were confirmed to be *Ntla*-dependent by *in situ* hybridization.

Entry	Gene symbol	Gene description	Expression domain at 10 hpf*	Fold change
1	<i>si:ch211-215a10.5-001 (hpcal4)</i>	novel protein similar to vertebrate hippocalcin like 4	<b>Axial</b>	-6.543
2	<i>LOC563543 (inpp5b)</i>	novel protein similar to vertebrate inositol polyphosphate-5-phosphatase	<b>Axial</b>	-6.093
3	<i>snai2</i>	snail homolog 2	<b>Axial</b>	-5.700
4	<i>LOC566628 (pskh2)</i>	novel protein similar to vertebrate protein serine kinase H2	<b>Axial</b>	-4.616
5	<i>lrrc8da</i>	novel protein similar to vertebrate leucine rich repeat containing 8 family, member D alpha	<b>Axial</b>	-4.602
6	<i>zgc:91787 (b3gnt7)</i>	novel protein similar to vertebrate beta-3-galactosyltransferase	<b>Axial</b>	-4.215
7	<i>col8a1a</i>	collagen, type VIII, alpha 1	<b>Axial</b>	-4.113
8	<i>plod1a</i>	lysyl hydroxylase 1	<b>Axial</b>	-3.848
9	<i>mnx1</i>	motor neuron and pancreas homeobox 1	<b>Axial</b>	-3.252
10	<i>pak1</i>	P21/Cdc42/Rac1-activated kinase 1	<b>Axial</b>	-3.114
11	<i>hdr</i>	hematopoietic death receptor	Axial	-2.773
12	<i>rgmb</i>	RGM domain family, member B	Axial	-2.721
13	<i>trpv4</i>	transient receptor potential cation channel, subfamily V, member 4	Axial	-2.712
14	<i>tacc2</i>	transforming, acidic coiled-coil containing protein 2	<b>Axial</b>	-2.693
15	<i>p4ha1</i>	procollagen-proline, 2-oxoglutarate 4-dioxygenase (proline 4-hydroxylase), alpha polypeptide I	<b>Axial</b>	-2.512
16	<i>hfe2</i>	hemochromatosis type 2	Axial	-2.485
17	<i>lrch2</i>	leucine-rich repeats and calponin homology (CH) domain containing 2	<b>Axial</b>	-2.431
18	<i>lipg</i>	lipase, endothelial	Axial	-2.429
19	<i>zgc:92198 (camk2n2)</i>	novel protein similar to vertebrate Ca <sup>2+</sup> /calmodulin-dependent protein kinase II inhibitor 2	Axial	-2.367
20	<i>fadd</i>	fas (tnfrsf6)-associated via death domain	Axial	-2.341
21	<i>twist2</i>	twist 2	Axial	-2.333
22	<i>hmcn1</i>	hemicentin 1	Axial	-2.272
23	<i>irx3a</i>	iroquois homeobox protein 3a	Axial	-2.242
24	<i>sall1a</i>	sal-like 1a	Axial	-2.206
25	<i>inka1a</i>	induced in neural crest by AP2, 1a	Axial	-2.17
26	<i>prickle2</i>	prickle-like 2	<b>Axial</b>	-2.135
27	<i>wwp2</i>	WW domain containing E3 ubiquitin protein ligase 2	Axial	-2.121

28	<i>id:ibd2573 (creb3l1)</i>	novel protein similar to vertebrate cAMP responsive element binding protein 3-like 1	Axial	-2.021
29	<i>tnfrsfa</i>	tumor necrosis factor receptor superfamily, member a	Axial	-2.013
30	<i>lhx1a</i>	LIM-homeobox 1a	<b>Axial</b> , Other	-6.092
31	<i>notch1b</i>	notch homolog 1b	<b>Axial</b> , Other	-5.524
32	<i>kirrel3l</i>	kin of IRRE like 3 like	<b>Axial</b> , Other	-3.334
33	<i>zgc:66052 (tagln3b)</i>	novel protein similar to vertebrate transgelin 3	Axial, Other	-2.939
34	<i>zgc:66433 (KIAA1211)</i>	novel protein similar to vertebrate uncharacterized protein KIAA1211	Axial, Other	-2.200
34/55 (62%) with axial expression				
35	<i>myod1</i>	myogenic determination factor 1	<b>Paraxial</b>	-4.290
36	<i>plp2</i>	proteolipid protein 2	Paraxial	-4.036
37	<i>cpn1</i>	carboxypeptidase N, polypeptide 1	Paraxial	-3.379
38	<i>aldh1a2</i>	aldehyde dehydrogenase 1 family, member A2	<b>Paraxial</b>	-3.255
39	<i>ppargc1al</i>	peroxisome proliferator activated receptor gamma coactivator 1 alpha - like	Paraxial	-3.026
40	<i>unc45b</i>	homolog of <i>C. elegans</i> unc-45B	<b>Paraxial</b>	-3.013
41	<i>myf5</i>	myogenic factor 5	Paraxial	-2.788
42	<i>smyd1b</i>	SET and MYND domain containing 1b	Paraxial	-2.532
43	<i>ttna</i>	titin a	Paraxial	-2.415
44	<i>ttnb</i>	titin b	Paraxial	-2.327
45	<i>meis4.1a</i>	myeloid ecotropic viral integration site 4.1a	Paraxial	-2.155
46	<i>dlc</i>	deltaC	Paraxial	-2.146
47	<i>notch2</i>	notch homolog 2	Paraxial	-2.072
13/55 (24%) with paraxial expression				
48	<i>wnt8a</i>	wingless-type MMTV integration site family, member 8a	<b>Tailbud</b> , Other	-4.652
49	<i>rbm38</i>	RNA binding motif protein 38	<b>Tailbud</b> , Paraxial	-3.483
50	<i>adora2ab</i>	adenosine receptor A2a.2	Tailbud, Other	-2.677
51	<i>her1</i>	hairy-related 1	<b>Tailbud</b> , <b>Paraxial</b>	-2.529
52	<i>tbx6</i>	T-box gene 6	<b>Tailbud</b> , Paraxial	-2.919
53	<i>wnt3l</i>	wingless-type MMTV integration site family, member 3 like	<b>Tailbud</b> <sup>4</sup> , Paraxial	-2.338
54	<i>st3gal2l</i>	ST3 beta-galactoside alpha-2,3-sialyltransferase 2, like	Tailbud, Paraxial	-2.321
55	<i>fgf24</i>	fibroblast growth factor 24	Tailbud, Paraxial	-2.020
8/55 (14%) with tailbud expression				
25/25 (100%) shown to have Ntla-dependent expression by <i>in situ</i> hybridization				

**Supplementary Table 5. cFD vs. *ntla* cMO + cFD comparison at 16 hpf: 9 microarray hits with known expression patterns, grouped by their expression domain at 16 hpf and ranked by fold change.**

\*Expression domains in highlighted in bold font were confirmed to be *Ntla*-dependent *in situ* hybridization.

Entry	Gene symbol	Gene description	Expression domain at 16 hpf*	Fold change
1	<i>LOC795255 (slc38a8)</i>	novel protein similar to vertebrate soluble carrier family 38 protein	<b>Axial</b>	-4.917
2	<i>znf385b</i>	zinc finger protein 385b	<b>Axial</b>	-2.357
3	<i>tspan7b</i>	tetraspanin 7b	<b>Axial</b>	-2.318
4	<i>ptrfb</i>	polymerase I and transcript release factor b	<b>Axial</b>	-2.046
5	zgc:110418 ( <i>kcnk6</i> )	novel protein similar to vertebrate potassium inwardly-rectifying channel, subfamily K, member 6	<b>Axial</b>	-2.030
6	<i>frzb</i>	frizzled-related protein	<b>Axial</b>	+3.320
7	<i>ntla</i>	no tail-a	<b>Axial</b>	+2.225
8	<i>cav3</i>	caveolin 3	<b>Axial, Paraxial</b>	-2.717
9	<i>wu:fd47f06 (guca2b)</i>	novel protein similar to vertebrate guanylate cyclase activator 2b	Ectoderm	+2.095
8/9 (89 %) with axial expression				

**Supplementary Table 6. cFD vs. *ntla* cMO comparison at 9 hpf: 87 microarray hits grouped by cellular function and ranked by fold change.**

Entry	Gene symbol	Gene description	Cellular function	Fold change
1	<i>hdr</i>	hematopoietic death receptor	Apoptosis	-2.773
2	<i>fadd</i>	fas (tnfrsf6)-associated via death domain	Apoptosis	-2.341
3	<i>tnfaip6</i>	tumor necrosis factor, alpha-induced protein 6	Apoptosis	-2.200
4	<i>tnfrsfa</i>	tumor necrosis factor receptor superfamily, member a	Apoptosis	-2.013
4/87 (5%) apoptosis				
5	<i>lrrc8da</i>	novel protein similar to vertebrate leucine rich repeat containing 8 family, member D alpha	Cell adhesion/migration	-4.602
6	<i>zgc:91787 (b3gnt7)</i>	novel protein similar to vertebrate beta-3-galactosyltransferase	Cell adhesion/migration	-4.215
7	<i>kirrel3l</i>	kin of IRRE like 3 like	Cell adhesion/migration	-3.334
8	<i>pak1</i>	P21/Cdc42/Rac1-activated kinase 1	Cell adhesion/migration	-3.114
9	<i>zgc:66052 (tagln3b)</i>	novel protein similar to vertebrate transgelin 3	Cell adhesion/migration	-2.939
10	<i>zgc:163023 (tspan4)</i>	novel protein similar to vertebrate tetraspanin 4	Cell adhesion/migration	-2.460
11	<i>itgb5</i>	integrin, beta 5	Cell adhesion/migration	-2.400
12	<i>st3gal2l</i>	ST3 beta-galactoside alpha-2,3-sialyltransferase 2, like	Cell adhesion/migration	-2.321
13	<i>hmcn1</i>	hemicentin 1	Cell adhesion/migration	-2.272
14	<i>inka1a</i>	induced in neural crest by AP2, 1a	Cell adhesion/migration	-2.170
10/87 (12%) cell adhesion/migration				
15	<i>si:ch211-215a10.5-001 (hpcal4)</i>	novel protein similar to vertebrate hippocalcin like 4	Cell signaling	-6.543
16	<i>LOC563543 (inpp5b)</i>	novel protein similar to vertebrate inositol polyphosphate-5-phosphatase	Cell signaling	-6.093
17	<i>notch1b</i>	notch homolog 1b	Cell signaling	-5.524
18	<i>wnt8a</i>	wingless-type MMTV integration site family, member 8a	Cell signaling	-4.652
19	<i>LOC566628 (pskh2)</i>	novel protein similar to vertebrate protein serine kinase H2	Cell signaling	-4.616
20	<i>pip5k1c</i>	phosphatidylinositol-4-phosphate 5-kinase, type I, gamma	Cell signaling	-3.592
21	<i>pde4ba</i>	cAMP-specific 3',5'-cyclic phosphodiesterase 4B alpha	Cell signaling	-3.547
22	<i>aldh1a2</i>	aldehyde dehydrogenase 1 family, member A2	Cell signaling	-3.255
23	<i>rgmb</i>	RGM domain family, member B	Cell signaling	-2.721
24	<i>trpv4</i>	transient receptor potential cation channel, subfamily V, member 4	Cell signaling	-2.712
25	<i>adora2ab</i>	adenosine receptor A2a.2	Cell signaling	-2.677
26	<i>zgc:153027 (esm1)</i>	novel protein similar to vertebrate endothelial cell-specific molecule 1	Cell signaling	-2.637
27	<i>kidins220a</i>	kinase D-interacting substance of 220 kDa	Cell signaling	-2.603
28	<i>zgc:92198 (camk2n2)</i>	novel protein similar to vertebrate Ca <sup>2+</sup> /calmodulin-dependent protein kinase II inhibitor 2	Cell signaling	-2.367
29	<i>wnt3l</i>	wingless-type MMTV integration site family, member 3 like	Cell signaling	-2.338
30	<i>dlc</i>	deltaC	Cell signaling	-2.146

31	<i>kitlga</i>	kit ligand a	Cell signaling	-2.145
32	<i>kif1b</i>	kinesin family member 1B	Cell signaling	-2.085
33	<i>notch2</i>	notch homolog 2	Cell signaling	-2.072
34	<i>fgf24</i>	fibroblast growth factor 24	Cell signaling	-2.020
35	<i>zgc:165655</i>	novel pleckstrin domain protein	Cell signaling	-2.009
36	<i>pdgfrb2</i>	platelet-derived growth factor receptor beta 1.2 fragment	Cell signaling	+2.442
22/87 (25%) cell signaling				
37	<i>plp2</i>	proteolipid protein 2	Endocytosis	-4.036
38	<i>sort1b</i>	sortilin 1, like	Endocytosis	-2.284
2/87 (2%) endocytosis				
39	<i>col8a1a</i>	collagen, type VIII, alpha 1	Extracellular matrix	-4.113
40	<i>plod1a</i>	lysyl hydroxylase 1	Extracellular matrix	-3.848
41	<i>cpn1</i>	carboxypeptidase N, polypeptide 1	Extracellular matrix	-3.379
42	<i>p4ha1</i>	procollagen-proline, 2-oxoglutarate 4-dioxygenase (proline 4-hydroxylase), alpha polypeptide I	Extracellular matrix	-2.512
4/87 (5%) extracellular matrix				
43	<i>lhx1a</i>	LIM-homeobox 1a	Gene expression	-6.092
44	<i>snai2</i>	snail homolog 2	Gene expression	-5.700
45	<i>si:dkey-49o11.4 (tbx3l)</i>	novel protein similar to vertebrate t-box 3	Gene expression	-5.072
46	<i>myod1</i>	myogenic determination factor 1	Gene expression	-4.290
47	<i>rbm38</i>	RNA binding motif protein 38	Gene expression	-3.483
48	<i>mnx1</i>	motor neuron and pancreas homeobox 1	Gene expression	-3.252
49	<i>hmbox1b</i>	similar to homeobox containing 1	Gene expression	-3.133
50	<i>tbx6</i>	T-box gene 6	Gene expression	-2.919
51	<i>myf5</i>	myogenic factor 5	Gene expression	-2.788
52	<i>si:dkey-195c14.1 (sall3l)</i>	novel protein similar to vertebrate sal-like 3	Gene expression	-2.552
53	<i>smyd1b</i>	SET and MYND domain containing 1b	Gene expression	-2.532
54	<i>her1</i>	hairy-related 1	Gene expression	-2.529
55	<i>mesp2</i>	mesoderm posterior 2 homolog	Gene expression	-2.333
56	<i>twist2</i>	twist 2	Gene expression	-2.333
57	<i>irx3a</i>	iroquois homeobox protein 3a	Gene expression	-2.242
58	<i>sall1a</i>	sal-like 1a	Gene expression	-2.206
59	<i>meis4.1a</i>	myeloid ecotropic viral integration site 4.1a	Gene expression	-2.155
60	<i>prickle2</i>	prickle-like 2	Gene expression	-2.135
61	<i>si:ch211-285f17.1 (KIAA1217)</i>	novel protein similar to vertebrate sickle tail protein homolog	Gene expression	-2.0300
62	<i>id:ibd2573 (creb3l1)</i>	novel protein similar to vertebrate cAMP responsive element binding protein 3-like 1	Gene expression	-2.021

63	<i>hbp1</i>	HMG box-containing protein 1	Gene expression	+2.037
64	<i>rbms3</i>	RNA binding motif, single stranded interacting protein	Gene expression	+2.095
22/87 (25%) gene expression				
65	<i>hfe2</i>	hemochromatosis type 2	Other (homeostasis)	-2.485
66	<i>lipg</i>	lipase, endothelial	Other (homeostasis)	-2.429
67	<i>nmnat2</i>	nicotinamide nucleotide adenyltransferase 2	Other (homeostasis)	+2.027
68	<i>atp1a1b</i>	ATPase, Na <sup>+</sup> /K <sup>+</sup> transporting, alpha 1b polypeptide	Other (membrane transporter)	-4.371
69	<i>abcc6b</i>	ATP-binding cassette, sub-family C, member 6b	Other (membrane transporter)	-3.344
70	<i>lamp1</i>	lysosomal-associated membrane protein 1	Other (protein homeostasis)	-3.426
71	<i>hspa12a</i>	heat shock 70 kDa protein 12A	Other (protein homeostasis)	-2.660
72	<i>wwp2</i>	WW domain containing E3 ubiquitin protein ligase 2	Other (protein homeostasis)	-2.121
73	<i>ube2e3</i>	ubiquitin-conjugating enzyme E2E 3	Other (protein homeostasis)	-2.120
9/87 (10%) other				
74	<i>ppargc1a</i>	peroxisome proliferator activated receptor gamma coactivator 1 alpha - like	Sarcomere assembly	-3.026
75	<i>unc45b</i>	homolog of <i>C. elegans</i> unc-45B	Sarcomere assembly	-3.013
76	<i>ttna</i>	titin a	Sarcomere assembly	-2.415
77	<i>actn2</i>	actinin, alpha 2	Sarcomere assembly	-2.384
78	<i>ttnb</i>	titin b	Sarcomere assembly	-2.327
79	<i>myom3</i>	myomesin family, member 3	Sarcomere assembly	+2.002
6/87 (7%) sarcomere assembly				
80	<i>si:dkey-146l2.1-001 (ankrd15)</i>	novel protein similar to vertebrate ankyrin repeat domain 15	Unknown	-4.281
81	<i>ribc1</i>	RIB43A domain with coiled-coils 1	Unknown	-3.614
82	<i>dopey2</i>	dopey family member 2	Unknown	-3.341
83	<i>caskin1</i>	CASK-interacting protein 1	Unknown	-3.206
84	<i>tacc2</i>	transforming, acidic coiled-coil containing protein 2	Unknown	-2.693
85	<i>lrch2</i>	leucine-rich repeats and calponin homology (CH) domain containing 2	Unknown	-2.431
86	<i>zgc:66433 (KIAA1211)</i>	novel protein similar to vertebrate uncharacterized protein KIAA1211	Unknown	-2.200
87	<i>ENSDARG0000006307 5 (c20orf117)</i>	novel protein similar to vertebrate uncharacterized protein c20orf117	Unknown	-2.1200
8/87 (9%) unknown				

**Supplementary Table 7. cFD vs. *ntl*a cMO + cFD comparison at 16 hpf: 12 microarray hits grouped by cellular function and ranked by fold change.**

Entry	Gene symbol	Gene description	Cellular function	Fold change
1	<i>tspan7b</i>	tetraspanin 7b	Cell adhesion/migration	-2.318
1/12 (8%) cell adhesion/migration				
2	<i>si:dkey-205o12.2 (prk1)</i>	novel protein similar to vertebrate pim oncogene related kinase 1	Cell signaling	-2.073
3	<i>frzb</i>	frizzled-related protein	Cell signaling	+3.320
4	<i>wu:fd47f06 (guca2b)</i>	novel protein similar to vertebrate guanylate cyclase activator 2b	Cell signaling	+2.095
3/12 (25%) cell signaling				
5	<i>LOC795255 (slc38a8)</i>	novel protein similar to vertebrate soluble carrier family 38 protein	Endocytosis	-4.917
6	<i>cav3</i>	caveolin 3	Endocytosis	-2.717
7	<i>ptrfb</i>	polymerase I and transcript release factor b	Endocytosis	-2.046
3/12 (25%) endocytosis				
8	<i>znf385b</i>	zinc finger protein 385b	Gene expression	-2.357
9	<i>si:dkeyp-122e7.1 (znf804a)</i>	novel protein similar to vertebrate zinc finger 804a	Gene expression	-2.051
10	<i>zgc:174919</i>	novel protein containing zinc finger domain	Gene expression	-2.039
11	<i>ntl</i> a	no tail-a	Gene expression	+2.225
4/12 (33 %) gene expression				
12	<i>zgc:110418 (kcnk6)</i>	novel protein similar to vertebrate potassium inwardly-rectifying channel, subfamily K, member 6	Membrane transporter	-2.030
1/12 (8%) other				



**Supplementary Table 8. cFD vs. *ntla* cMO + cFD comparison at 9 hpf: 34 microarray hits with reported loss-of-function studies, grouped by their expression domain at 10 hpf and ranked by phenotype and fold change.**

\*Expression domains highlight in bold font were confirmed to be *Ntla*-dependent by *in situ* hybridization.

\*\*Loss-of-function methods highlighted in bold font were performed in this study.

\*\*\*Phenotypes related to mesodermal patterning are indicated. Those highlighted in bold font were investigated in this study.

Entry	Gene symbol	Gene description	Expression domain at 10 hpf*	Fold Change	Loss-of-function method**	Mesodermal defects***
1	<i>pak1</i>	P21/Cdc42/Rac1-activated kinase 1	<b>Axial</b>	-3.114	Morpholino	Gastrulation <sup>5</sup>
2	<i>irx3a</i>	iroquois homeobox protein 3a	Axial	-2.242	Morpholino	Gastrulation <sup>6</sup>
3	<i>prickle2</i>	prickle-like 2	<b>Axial</b>	-2.135	Morpholino	Gastrulation <sup>7</sup>
4	<i>col8a1a</i>	collagen, type VIII, alpha 1	<b>Axial</b>	-4.113	Mutant, <b>Morpholino</b>	<b>Notochord</b> <sup>8</sup>
5	<i>mnx1</i>	motor neuron and pancreas homeobox 1	<b>Axial</b>	-3.252	<b>Morpholino</b>	<b>Notochord, Muscle</b>
6	<i>si:ch211-215a10.5-001 (hpcal4)</i>	novel protein similar to vertebrate hippocalcin like 4	<b>Axial</b>	-6.543	<b>Morpholino</b>	<b>None</b>
7	<i>LOC563543 (inpp5b)</i>	novel protein similar to vertebrate inositol polyphosphate-5-phosphatase	<b>Axial</b>	-6.093	<b>Morpholino</b>	<b>None</b>
8	<i>snai2</i>	snail homolog 2	<b>Axial</b>	-5.700	<b>Morpholino</b>	<b>None</b>
9	<i>hdr</i>	hematopoietic death receptor	Axial	-2.773	Morpholino	None <sup>9</sup>
10	<i>trpv4</i>	transient receptor potential cation channel, subfamily V, member 4	Axial	-2.712	Mutant, Morpholino	None <sup>10</sup>
11	<i>tacc2</i>	transforming, acidic coiled-coil containing protein 2	<b>Axial</b>	-2.693	<b>Morpholino</b>	<b>None</b>
12	<i>fadd</i>	fas (tnfrsf6)-associated via death domain	Axial	-2.341	Morpholino	None <sup>9</sup>
13	<i>hmcn1</i>	hemicentin 1	Axial	-2.272	Mutant	None <sup>11,12</sup>
14	<i>sall1a</i>	sal-like 1a	Axial	-2.206	Morpholino	None <sup>13</sup>
15	<i>inka1a</i>	induced in neural crest by AP2, 1a	Axial	-2.170	Mutant, Morpholino	None <sup>14</sup>
16	<i>tnfrsfa</i>	tumor necrosis factor receptor superfamily, member a	Axial	-2.013	Morpholino	None <sup>9</sup>
17	<i>kirrel3l</i>	kin of IRRE like 3 like	<b>Axial, Other</b>	-3.334	Morpholino	Muscle <sup>15</sup>
18	<i>lhx1a</i>	LIM-homeobox 1a	<b>Axial, Other</b>	-6.092	<b>Morpholino</b>	<b>None</b>
19	<i>notch1b</i>	notch homolog 1b	<b>Axial, Other</b>	-5.524	Morpholino	None <sup>16-18</sup>
2/19 (10%) with axial expression had notochord defects						
20	<i>myod1</i>	myogenic determination factor 1	<b>Paraxial</b>	-4.290	Mutant, Morpholino	Muscle <sup>19</sup>
21	<i>unc45b</i>	homolog of <i>C. elegans</i> unc-45B	<b>Paraxial</b>	-3.013	Mutant, Morpholino	Muscle <sup>20</sup>

22	<i>myf5</i>	myogenic factor 5	Paraxial	-2.788	Mutant, Morpholino	Muscle <sup>21</sup>
23	<i>smyd1b</i>	SET and MYND domain containing 1b	Paraxial	-2.532	Morpholino	Muscle <sup>22</sup>
24	<i>ttna</i>	titin a	Paraxial	-2.415	Mutant, Morpholino	Muscle <sup>23</sup>
25	<i>ttnb</i>	titin b	Paraxial	-2.327	Morpholino	Muscle <sup>23</sup>
26	<i>dlc</i>	deltaC	Paraxial	-2.146	Mutant, Morpholino	Muscle <sup>24</sup>
27	<i>aldh1a2</i>	aldehyde dehydrogenase 1 family, member A2	<b>Paraxial</b>	-3.255	Mutant, Morpholino	No <sup>25,26</sup>
28	<i>meis4.1a</i>	myeloid ecotropic viral integration site 4.1a	Paraxial	-2.155	Morpholino	None <sup>27</sup>
29	<i>notch2</i>	notch homolog 2	Paraxial	-2.072	Morpholino	None <sup>16</sup>
7/10 (70%) with paraxial expression had muscle defects						
30	<i>wnt8a</i>	wingless-type MMTV integration site family, member 8a	<b>Tailbud, Other</b>	-4.652	Mutant, Morpholino	Notochord, Mesoderm <sup>28-30</sup>
31	<i>wnt3l</i>	wingless-type MMTV integration site family, member 3 like	<b>Tailbud, Paraxial</b>	-2.338	Morpholino	Mesoderm <sup>29,30</sup>
32	<i>fgf24</i>	fibroblast growth factor 24	Tailbud, Paraxial	-2.020	Mutant, Morpholino	Mesoderm <sup>31</sup>
33	<i>ppargc1a1</i>	peroxisome proliferator activated receptor gamma coactivator 1 alpha - like	Paraxial	-3.026	Morpholino	Muscle <sup>32</sup>
34	<i>her1</i>	hairy-related 1	<b>Tailbud, Paraxial</b>	-2.529	Mutant, Morpholino	Muscle <sup>33</sup>
3/5 (60%) with tailbud expression had mesoderm defects						

**Supplementary Table 9. cFD vs. *ntla* cMO + cFD comparison at 16 hpf: 4 microarray hits with reported loss-of-function studies, grouped by their expression domain at 16 hpf and ranked by fold change.**

\*Expression domains highlighted in bold font were confirmed to be *Ntla*-dependent by *in situ* hybridization.

\*\*Phenotypes highlighted in bold font were investigated in this study.

Entry	Gene symbol	Gene description	Expression domain at 16 hpf*	Fold Change	Loss-of-function method	Notochord defects**
1	<i>LOC795255 (slc38a8)</i>	novel protein similar to vertebrate soluble carrier family 38 protein	<b>Chordamesoderm</b>	-4.917	Morpholino	<b>Yes</b>
2	<i>znf385b</i>	zinc finger protein 385b	<b>Chordamesoderm</b>	-2.357	Morpholino	<b>Yes</b>
3	<i>ptrfb</i>	polymerase I and transcript release factor b	<b>Chordamesoderm</b>	-2.046	Morpholino	<b>Yes</b> <sup>34</sup>
4	<i>cav3</i>	caveolin 3	<b>Chordamesoderm, Paraxial</b>	-2.717	Morpholino	<b>Yes</b> <sup>35</sup>

### Supplementary Table 10. MO sequences and doses.

\*Bases complementary to start codons are underlined, where appropriate.

\*\*Intron/exon assignments are based upon the zebrafish genome assembly Zv8, gene build 59 (May 2010).

MO	Sequence*	Targeted region**	Dose (per embryo)	Functional validation
<i>cav3</i> MO	CGTTAGTGTGTACTGGTCCGCCAT	translational start site	3 ng + 4.5 ng <i>tp53</i> MO	previously reported morphant <sup>35</sup>
<i>col8a1a</i> MO	CCGTAGGAGAAGATAATCTCAAGGA	translational start site	6 ng	mutant phenocopy <sup>8</sup>
<i>lhx1a</i> MO1	CCCGCACAGTGGACCATCGTCTTTG	translational start site	18 ng	
<i>lhx1a</i> MO2	GACCATCGTCTTTGGATGTGCTCCC	translational start site	8 ng	
<i>LOC563543 (inpp5b)</i>	CTGGAAACTACCGGAGGAAAACACA	splice - i9e10	3 ng + 4.5 ng <i>tp53</i> MO	missplicing – Supp. Fig. 6C
<i>LOC795255 (slc38a8)</i> MO1	TGGCATAGCCTCTAACACACCTGGT	splice - e3i3	6 ng	missplicing – Supp. Fig. 8G
<i>LOC795255 (slc38a8)</i> MO2	AGTTCCTCCATCCTCAGCGCCTCAA	translational start site	1.5 ng + 2.2 ng <i>tp53</i> MO	phenocopy of MO1
<i>mnx1</i> MO1	GCCTGGCCTGCATGGAGAATTTTAA	splice - i1e2	9 ng	missplicing – Supp. Fig. 5D
<i>mnx1</i> MO2	AAAAGAAAGGTTTACCTGCGTCTCT	splice - e2i2	6 ng	missplicing – Supp. Fig. 5D
<i>ntlA</i> cMO	GACTTGAGGCAGACATATTTCCGAT-linker-GCCTCAAGTC	cMO	1.5 ng	mutant phenocopy <sup>36,37</sup>
<i>ntlA</i> MO	GACTTGAGGCAGACATATTTCCGAT	translational start site	1 ng	mutant phenocopy <sup>36,37</sup>
<i>ptrfb</i> MO	GACGGCTGTCTTCAATCACCTCCAT	translational start site	6 ng	previously reported morphant <sup>34</sup>
<i>si:ch211-215a10.5-001 (hpcal4)</i> MO1	GTTTTCCCATCTCTACACCTCACTG	translational start site	6 ng + 9 ng <i>tp53</i> MO	
<i>si:ch211-215a10.5-001 (hpcal4)</i> MO2	GCTTGCTGTTGTGTTTTCCCATCTC	translational start site	2 ng + 3 ng <i>tp53</i> MO	
<i>snai2</i>	ATACATGTCATTTTCTCACCCGTGT	splice - e2i2	3 ng	missplicing – Supp. Fig. 6E
<i>tacc2</i>	TCCATCTTTTGTCTCTTACCATCA	splice – e7i7	1 ng + 2 ng <i>tp53</i> MO	missplicing – Supp. Fig. 6F
<i>tp53</i> MO	GCGCCATTGCTTTGCAAGAATTG	translational start site	–	previously reported morphant <sup>38</sup>
<i>znf385b</i> MO1	TTCTGGAGGTCTTACCTTGACTGCT	splice - e2i2	3 ng + 4.5 ng <i>tp53</i> MO	missplicing – Supp. Fig. 8K
<i>znf385b</i> MO2	TGGCTCTACAAAGGAGAACAATGA	splice - i4e5	3 ng + 4.5 ng <i>tp53</i> MO	missplicing – Supp. Fig. 8K

**Supplementary Table 11. Phenotype statistics for morpholino experiments in order of presentation.**

Figure	Panel	Phenotypic criteria	Total number of embryos	Number with phenotype	% Penetrance
1	c, top	Fluorescent notochord and medial floor plate	20	20	100
1	c, bottom	Fluorescent medial floor plate alone	26	23	88
1	d, top	Fluorescent notochord and neural tube	29	29	100
1	d, bottom	Fluorescent, incompletely vacuolated notochord and neural tube	24	24	100
2	b	Axial and ventral mesoderm expression of <i>lhx1a</i>	21	21	100
2	c	Loss of axial expression of <i>lhx1a</i>	20	20	100
2	d	Axial expression of <i>mnx1</i>	18	18	100
2	e	Loss of axial expression of <i>mnx1</i>	21	21	100
2	f	Tailbud expression of <i>rbm38</i>	22	22	100
2	g	Loss of axial tailbud expression of <i>rbm38</i>	21	21	100
2	h	Adaxial expression of <i>unc45b</i>	17	17	100
2	i	Reduced adaxial expression of <i>unc45b</i>	23	20	87
2	j	Chordamesodermal and somitic expression of <i>cav3</i>	10	10	100
2	k	Reduced chordamesodermal expression of <i>cav3</i>	10	8	80
2	l	Chordamesodermal expression of <i>tspan7b</i>	12	12	100
2	m	Reduced chordamesodermal expression of <i>tspan7b</i>	12	12	100
2	n	Chordamesodermal expression of <i>slc38a8</i>	12	12	100
2	o	Reduced chordamesodermal expression of <i>slc38a8</i>	10	10	100
2	p	Chordamesodermal expression of <i>znf385b</i>	16	15	94
2	q	Reduced chordamesodermal expression of <i>znf385b</i>	10	8	80
3	c	Undulating notochord	37	37	100
3	d	Wildtype-like notochord	26	26	100
3	f	Somite patterning defects	24	24	100
3	g	Somite patterning defects	26	26	100
3	h	Axial expression of <i>shha</i>	20	20	100
3	i	Axial expression of <i>shha</i>	17	17	100
3	j	Axial expression of <i>ihhb</i>	20	20	100
3	k	Reduced axial expression of <i>ihhb</i>	20	20	100
3	l	Adaxial expression of <i>ptc1</i>	21	18	86
3	m	Adaxial expression of <i>ptc1</i>	18	16	89
3	o	Incomplete notochord vacuolization	16	12	75
3	p	Incomplete notochord vacuolization	18	9	50
S1	6 hpf	Ntla expression in the germ ring at wildtype level	8	8	100
S1	7 hpf	Ntla expression in the germ ring and axial mesoderm at wildtype level	8	6	75

S1	8 hpf	Ntla expression in axial mesoderm is reduced where co-localized with FD	8	8	100
S2	12 hpf	Ntla expression in the chordamesoderm at wildtype level	8	8	100
S2	14 hpf	Ntla expression in the chordamesoderm at nearly wildtype level	6	5	100
S2	16 hpf	Ntla expression in the chordamesoderm is reduced where co-localized with FD	7	7	100
S3	<i>aldh1a2</i> , WT	Paraxial expression	18	18	100
S3	<i>aldh1a2</i> , MO	Reduced paraxial expression	21	16	76
S3	<i>b3gnt7</i> , WT	Axial expression	34	34	100
S3	<i>b3gnt7</i> , MO	Loss of axial expression	33	33	100
S3	<i>col8a1a</i> , WT	Axial expression	22	21	95
S3	<i>col8a1a</i> , MO	Loss of axial expression	25	22	88
S3	<i>her1</i> , WT	Tailbud and paraxial expression	23	18	78
S3	<i>her1</i> , MO	Reduced tailbud expression	22	22	100
S3	<i>hpcal4</i> , WT	Axial expression	18	18	100
S3	<i>hpcal4</i> , MO	Loss of axial expression	16	16	100
S3	<i>inpp5b</i> , WT	Axial expression	18	18	100
S3	<i>inpp5b</i> , MO	Loss of axial expression	22	22	100
S3	<i>kirrel3l</i> , WT	Axial and anterior expression	22	22	100
S3	<i>kirrel3l</i> , MO	Loss of axial expression	37	37	100
S3	<i>lhx1a</i> , WT	Axial and lateral expression	18	14	78
S3	<i>lhx1a</i> , MO	Loss of axial expression	20	20	100
S3	<i>lrch2</i> , WT	Axial expression	22	20	91
S3	<i>lrch2</i> , MO	Loss of axial expression	20	20	100
S3	<i>lrrc8da</i> , WT	Axial expression	20	18	90
S3	<i>lrrc8da</i> , MO	Loss of axial expression	21	20	95
S3	<i>mnx1</i> , WT	Axial expression	18	17	94
S3	<i>mnx1</i> , MO	Loss of axial expression	21	21	100
S3	<i>myod1</i> , WT	Adaxial expression	20	20	100
S3	<i>myod1</i> , MO	Reduced adaxial expression	28	28	100
S3	<i>notch1b</i> , WT	Axial, adaxial, tailbud, and anterior expression	19	19	100
S3	<i>notch1b</i> , MO	Loss of axial expression	14	14	100
S3	<i>p4ha1</i> , WT	Axial expression	21	20	95
S3	<i>p4ha1</i> , MO	Loss of axial expression	22	22	100
S3	<i>pak1</i> , WT	Axial expression	21	20	95
S3	<i>pak1</i> , MO	Loss of axial expression	23	23	100
S3	<i>plod1a</i> , WT	Axial expression	19	19	100
S3	<i>plod1a</i> , MO	Loss of axial expression	33	33	100
S3	<i>prickle2</i> , WT	Axial expression	17	17	100
S3	<i>prickle2</i> , MO	Loss of axial expression	35	33	94
S3	<i>pskh2</i> , WT	Axial expression	24	24	100

S3	<i>pskh2</i> , MO	Loss of axial expression	24	22	92
S3	<i>rbm38</i> , WT	Tailbud expression	22	22	100
S3	<i>rbm38</i> , MO	Reduced tailbud expression	21	21	100
S3	<i>snai2</i> , WT	Axial expression	17	17	100
S3	<i>snai2</i> , MO	Loss of axial expression	19	18	95
S3	<i>tacc2</i> , WT	Axial expression	18	17	94
S3	<i>tacc2</i> , MO	Loss of axial expression	17	17	100
S3	<i>tbx6</i> , WT	Paraxial expression	19	19	100
S3	<i>tbx6</i> , MO	Reduced paraxial expression	21	21	100
S3	<i>unc45b</i> , WT	Adaxial expression	17	17	100
S3	<i>unc45b</i> , MO	Reduced adaxial expression	23	20	87
S3	<i>wnt8a</i> , WT	Tailbud expression	19	19	100
S3	<i>wnt8a</i> , MO	Reduced tailbud expression	13	11	85
S4	<i>cav3</i> , WT	Chordamesodermal and somitic expression	9	9	100
S4	<i>cav3</i> , no UV	Chordamesodermal and somitic expression	10	10	100
S4	<i>cav3</i> , UV	Reduced chordamesodermal expression	10	8	80
S4	<i>frzb</i> , WT	No expression	11	11	100
S4	<i>frzb</i> , no UV	No expression	9	6	67
S4	<i>frzb</i> , UV	Chordamesodermal expression	9	9	100
S4	<i>guca2b</i> , WT	Ectodermal expression	11	11	100
S4	<i>guca2b</i> , no UV	Ectodermal expression	13	13	100
S4	<i>guca2b</i> , UV	Ectodermal expression	10	10	100
S4	<i>kcnk6</i> , WT	Chordamesodermal expression	18	18	100
S4	<i>kcnk6</i> , no UV	Chordamesodermal expression	12	12	100
S4	<i>kcnk6</i> , UV	Reduced chordamesodermal expression	12	12	100
S4	<i>ntla</i> , WT	Chordamesodermal expression	6	6	100
S4	<i>ntla</i> , no UV	Chordamesodermal expression	13	13	100
S4	<i>ntla</i> , UV	Increased chordamesodermal expression	6	6	100
S4	<i>ptrfb</i> , WT	Chordamesodermal expression	10	10	100
S4	<i>ptrfb</i> , no UV	Chordamesodermal expression	12	11	92
S4	<i>ptrfb</i> , UV	Reduced chordamesodermal expression	8	8	100
S4	<i>slc38a8</i> , WT	Chordamesodermal expression	9	9	100
S4	<i>slc38a8</i> , no UV	Chordamesodermal expression	12	12	100
S4	<i>slc38a8</i> , UV	Reduced chordamesodermal expression	10	10	100
S4	<i>tspan7b</i> , WT	Chordamesodermal expression	21	21	100
S4	<i>tspan7b</i> , no UV	Chordamesodermal expression	12	12	100
S4	<i>tspan7b</i> , UV	Reduced chordamesodermal expression	12	12	100
S4	<i>znf385b</i> , WT	Chordamesodermal expression	22	22	100
S4	<i>znf385b</i> , no UV	Chordamesodermal expression	16	15	94

S4	<i>znf385b</i> , UV	Reduced chordamesodermal expression	19	15	79
S5	b	Somite patterning defects	13	11	85
S5	c	Somite patterning defects	21	19	90
S5	e	U-shaped somites and ventral body curvature	17	17	100
S5	f	Somite patterning defects	24	24	100
S6	b, MO1	Ventral body curvature	24	19	79
S6	b, MO2	Ventral body curvature	19	11	58
S6	c	Mild necrosis throughout embryo	15	15	100
S6	d, MO1	Wildtype-like morphology	45	45	100
S6	d, MO2	Ventral body curvature	51	42	82
S6	e	Wildtype-like morphology	17	17	100
S6	f	Wildtype-like morphology	15	15	100
S7	<i>mnx1</i> , F59	Shortened slow muscle fibers	18	18	100
S7	<i>mnx1</i> , F310	Wildtype-like fast muscle fibers	21	21	100
S7	<i>ntla</i> , F59	Disorganized, shortened slow muscle fibers	23	23	100
S7	<i>ntla</i> , F310	Shortened fast muscle fibers	20	20	100
S7	<i>Cyc</i> , F59	Disorganized and fewer slow muscle fibers	26	26	100
S7	<i>Cyc</i> , F310	Wildtype-like fast muscle fibers	29	29	100
S8	b	Incomplete notochord vacuolization	35	34	97
S8	c	Reduced cell-cell contacts within the notochord	27	25	93
S8	d	Incomplete notochord vacuolization	16	12	75
S8	e	Incomplete notochord vacuolization	20	14	70
S8	f	Incomplete notochord vacuolization	21	14	67
S8	h	Incomplete notochord vacuolization	18	9	50
S8	i	Incomplete notochord vacuolization	21	8	38
S8	j	Incomplete notochord vacuolization	27	18	67
S9	a, 6-hpf UV	Wildtype-like <i>flh</i> expression	12	12	100
S9	b, 6-hpf UV	Wildtype-like <i>flh</i> expression	12	12	100

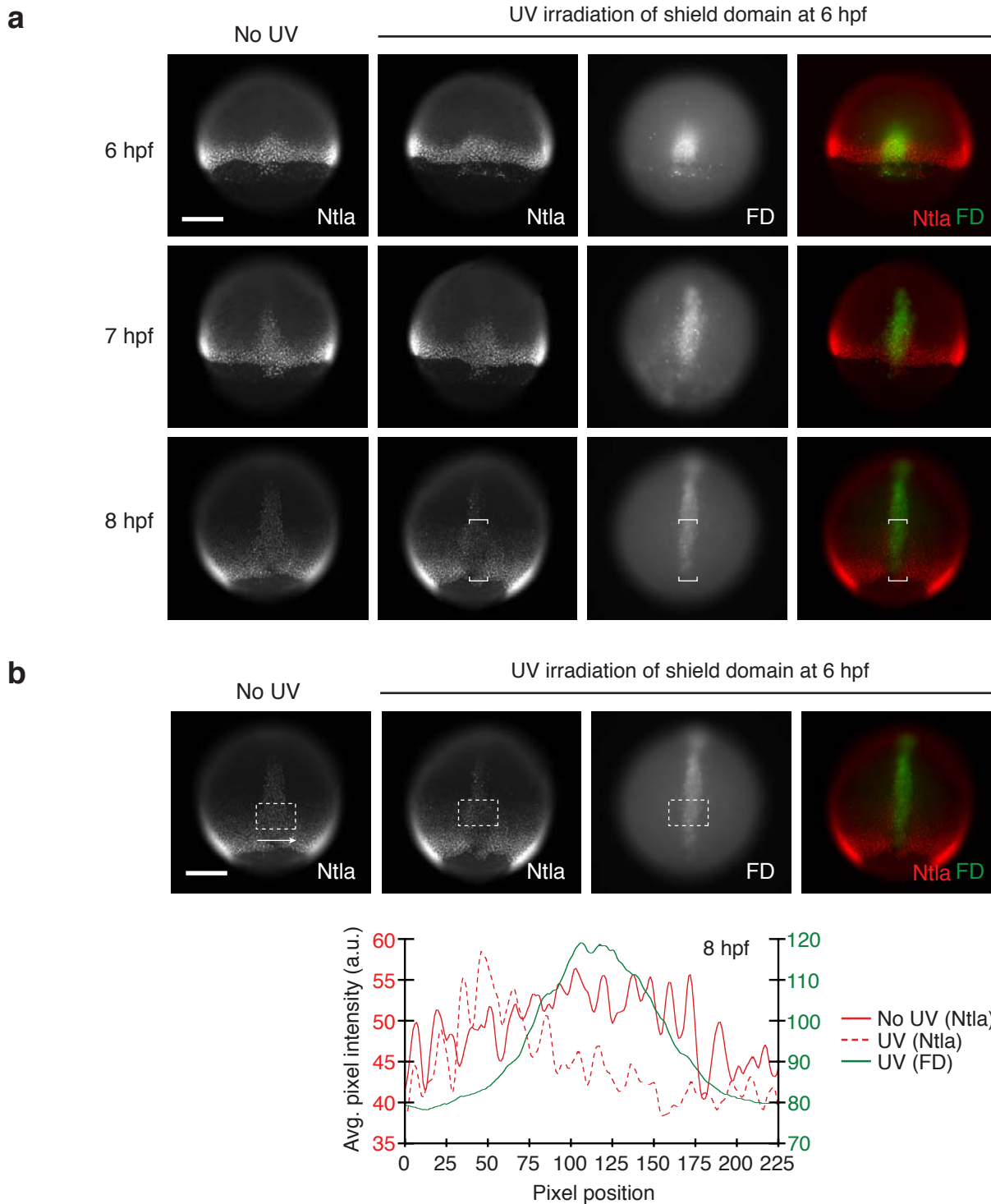


**Supplementary Table 12. Primer sequences used to verify MO-induced RNA missplicing.**

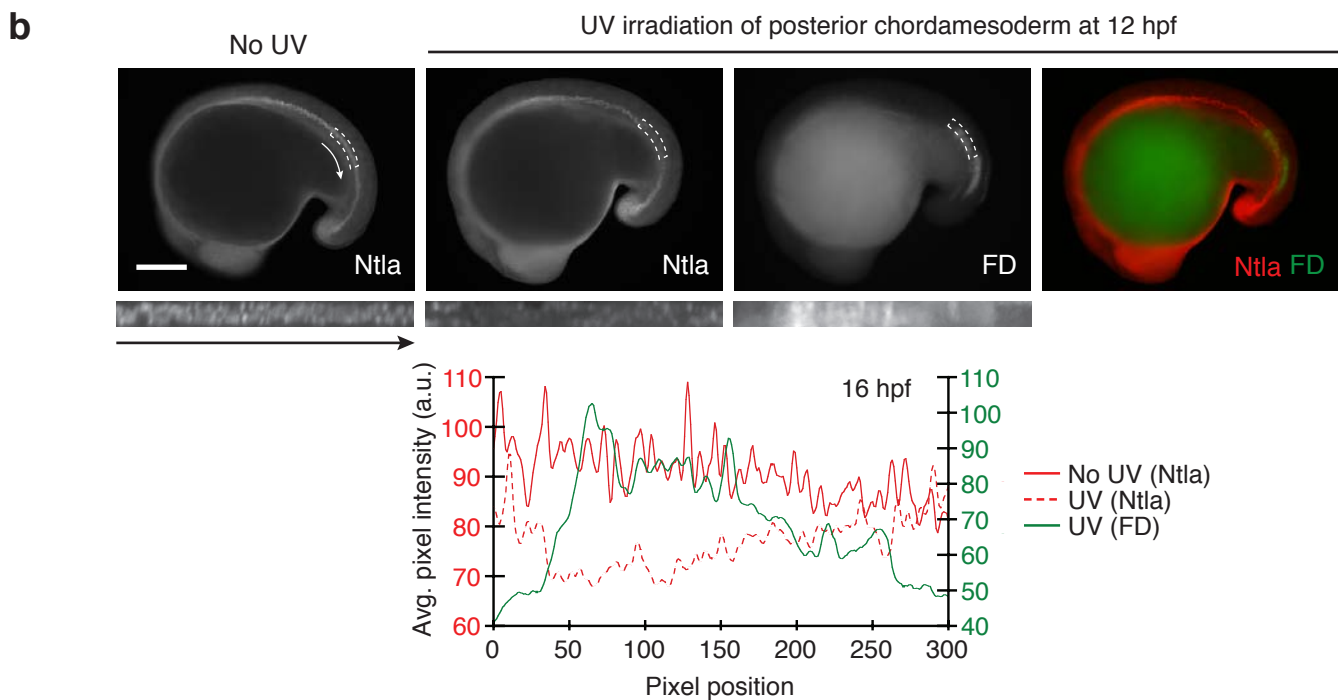
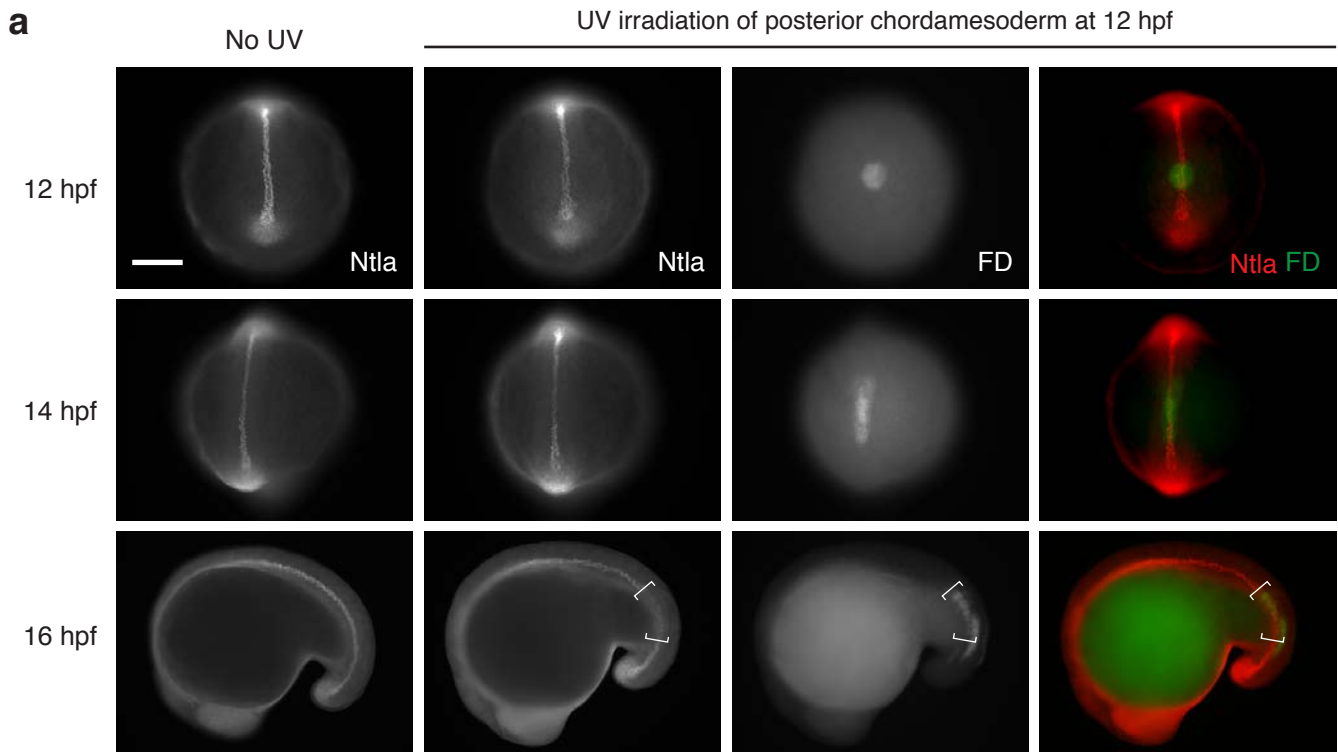
<b>Transcript</b>	<b>Forward</b>	<b>Reverse</b>
<i>LOC563543 (inpp5b)</i> MO	TTCGGCCTGCGGGATAACCTC	GAACTGGAAGCGGATGGAAACTGC
<i>LOC795255 (slc38a8)</i> MO1	AAGGCTGGCGGCGTGAACA	GAAGCCCATGAGCCCAATCCT
<i>mnx1</i> MO1 or MO2	CTCCCTGCCACCTCATCCAT	GGCCTTTTTACTGCGCTTCCATTTT
<i>snai2</i> MO	GGAAGATGAGGCTCTGCTGGAACG	CGATCTGCGAATGCACGACTGC
<i>tacc2</i> MO	ATGGCTCAATCAGTCCCTTCAAATCA	GCCCTTCGAAACGCTGCTGTC
<i>znf385</i> MO1	TGCAACACAGAGTGACGCCAAGTCT	ACCGCGGGCGCAACAGG
<i>znf385</i> MO2	CCGGTCGGCCTGTTCCCTAAT	GGTTTGCCTGCCACTCTGTCCTT

**Supplementary Table 13. Primer sequences used to generate *in situ* probes.**

Transcript	Forward	Reverse
<i>aldh1a2</i>	AGACGCGATGACCTCCAGTGAAGT	CCGAGGTAGAGGCAGGTGAGAGG
<i>cav3</i>	CGCCGCAGCTGTCTCTACCATT	AGGCCACCCGAACACTGCTAAAG
<i>col8a1a</i>	CCCGGGCCAAAAGGAGAAGTT	AACCCGGAGAAGGAGGAGTGGA
<i>frzb</i>	CTGGCCTTCGCATGTCTCCTG	TATCTGGCCCCTCCGCTTTGA
<i>her1</i>	CCAAAACCTCCGCCTCTGCTC	CCTGGGACGACCGGTAATGAAGT
<i>kirrel3l</i>	CTGCTGCCGCCACAATGCTAA	TCCCCGTCCGATTCCACATTC
<i>lhx1a</i>	CGGAGGGCACGGAGCAAAGT	GGGCCCCGAAAACATCTGAGGAC
<i>LOC563543 (inpp5b)</i>	ACTCGCATCTCGCCGCACAC	GAAGCAGCTGGGCAGGTAGGAG
<i>LOC566628 (pskh2)</i>	GGGCTGGCCTGTTGGGATAAGT	CCGGCGCTGGAGGTTTCTG
<i>LOC795255 (slc38a8)</i>	CTCATTGGGGCCATTTTCATCAT	AGTCGCAGCCAGAGTTCCCATTAC
<i>lrch2</i>	TGAACTGTCCGATCTGCCATTGA	TCAGCCCCTGCCGTTTCTG
<i>lrrc8da</i>	TGACCATTTGCGATGCCTACACA	TCTGGGATGCTGGTGATGTTGTTATG
<i>mnx1</i>	CTCCCTGCCACCTCATCCAT	GGCCTTTTTACTGCGTTCCATT
<i>notch1b</i>	ACGGGCGCACAGGTCTGTTG	ATCCCGTTTCGCAGGCACAC
<i>p4ha1</i>	AGCCGCCTGTTTTGCCGTTAC	ACTGCTGCTCCTACATCCGTGAAG
<i>pak1</i>	CCGCCCATGAGGAACACCAG	CCCCTGGCCGATCTTCTCAA
<i>plod1a</i>	CGCCCGCTCAGAGGATTATGTG	TGAAAGTGGAGGCGTCGTGATG
<i>prickle2</i>	CTGCGGGGAACACATCGGTATT	GTGGCCCAACATCCTTTTCTTC
<i>ptrfb</i>	GGAAGGGGAAGCTGAGGGTGAA	AGCGGGCGTAGATGGTGTGGT
<i>rbm38</i>	GGATAAAAGTGCAGCGGAAAGAGC	GGGTGGAGATGGCGGAGGAT
<i>si:ch211-215a10.5-001 (hpcal4)</i>	CAGCAAGCTGGCTCCTGAGGTG	TTTGGCCGTTCTTTGAACTCC
<i>snai2</i>	AGCGCTGGAAGATGAGGCTCTG	GCAGGTGGGCTCGGAGGTTTC
<i>tacc2</i>	CCAATCCCCAAGGCATCATAAAC	CGGTCCGCTGTGGGAAATCTT
<i>tbx6</i>	GGAACGGCCTGTGCTGGACTTA	ATGTGTAGACGGGGCTGGTATTTGTG
<i>tspan7b</i>	AGCGGAGGGAGGAAAGGCACTA	CAAAGGCAACAAAACCACCGATAAC
<i>unc45b</i>	GGCAGGTCGGCAGGGTGTAAT	GCAGGCGACCGCATACAGGAT
<i>wnt8a</i>	ATCGGAAAAATGGGTGGTTCGTG	GCCGCCTGCAGCTTCTTCTCT
<i>wu:fb47f06 (guca2b)</i>	CCGTCGCTTTCCTCGTCGTG	TGCAAGCCGCGAAAGCACA
<i>zgc:110418 (kcnk6)</i>	CGCCGGTAAAGCCTTCTCCATC	CCGTCCAGCCGTAACATCAGC
<i>zgc:91787 (b3gnt7)</i>	GCGGCGGCGTGGATGTT	GACTTTGCGGGCCACCTGAGA
<i>znf385b</i>	GAGGCACGAAATGGAGCAGGTC	GAGCGGCACGGAGAAACGAG

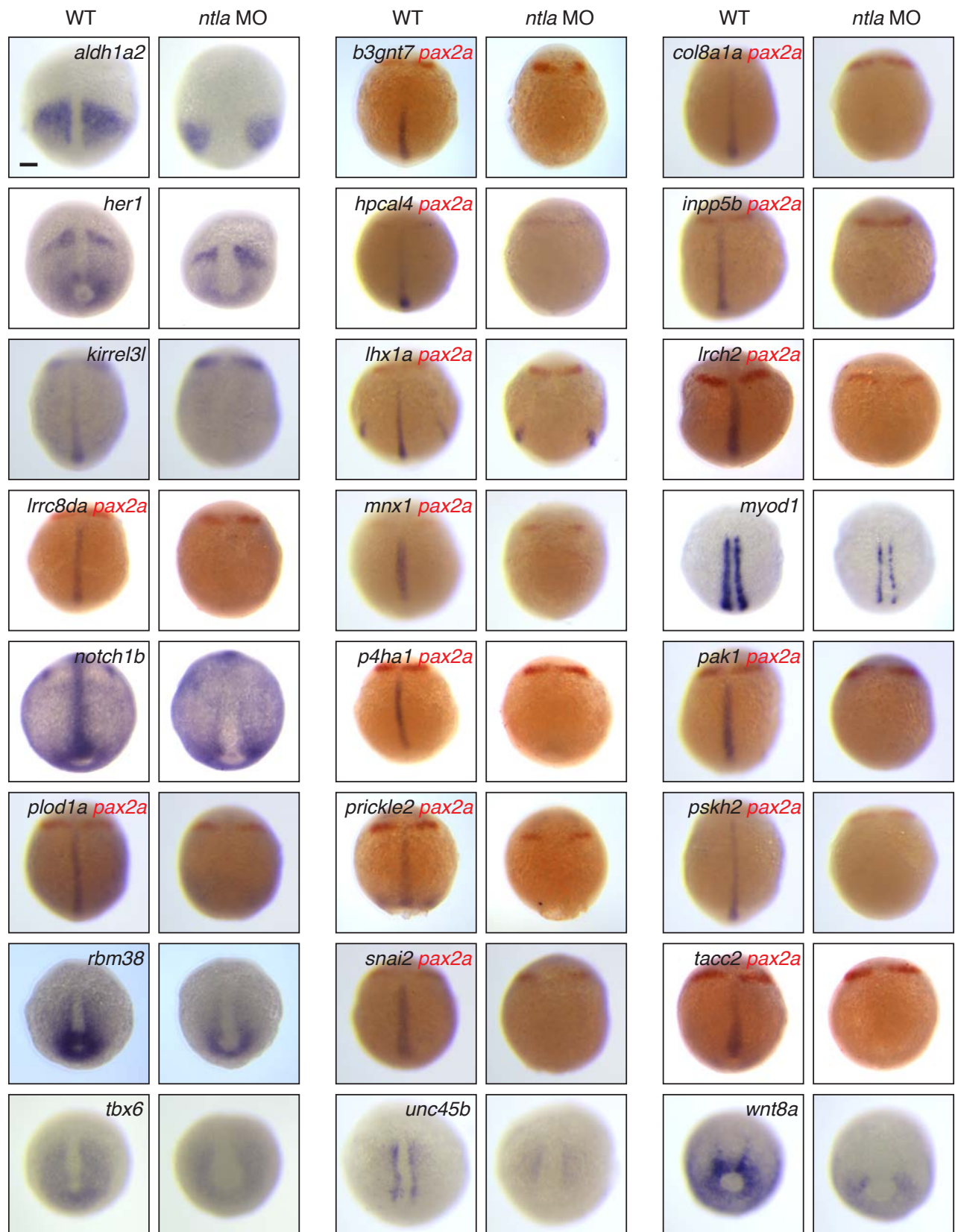


**Supplementary Figure 1. Ntla protein depletion after *ntla* cMO photoactivation within the embryonic shield.** **a**, Zebrafish zygotes were injected with a *ntla* caged morpholino (cMO)/caged fluorescein-conjugated dextran (cFD) mixture and then irradiated within a 100  $\mu$ m-diameter region centered on the shield domain at 6 hours post fertilization (hpf). The irradiated embryos fixed at various developmental time points were assessed by whole-mount immunostaining for Ntla and uncaged fluorescein-conjugated dextran (FD) levels. Non-irradiated embryos were processed and analyzed in an equivalent manner to provide a comparison control, and regions of Ntla protein depletion are indicated by the brackets. **b**, Quantification of Ntla protein levels in 8-hpf embryos after *ntla* cMO photoactivation. Regions demarcated by the dashed white lines were selected for quantification, and average pixel intensities for each position along the horizontal axis (arrow) were determined using ImageJ software. Pixel intensities for Ntla immunostaining in non-irradiated (red line) and locally irradiated (dashed red line) embryos are shown, as well as those for FD immunostaining in locally irradiated embryos (green line). Embryo orientations: dorsal view and anterior up. Scale bars: 200  $\mu$ m.

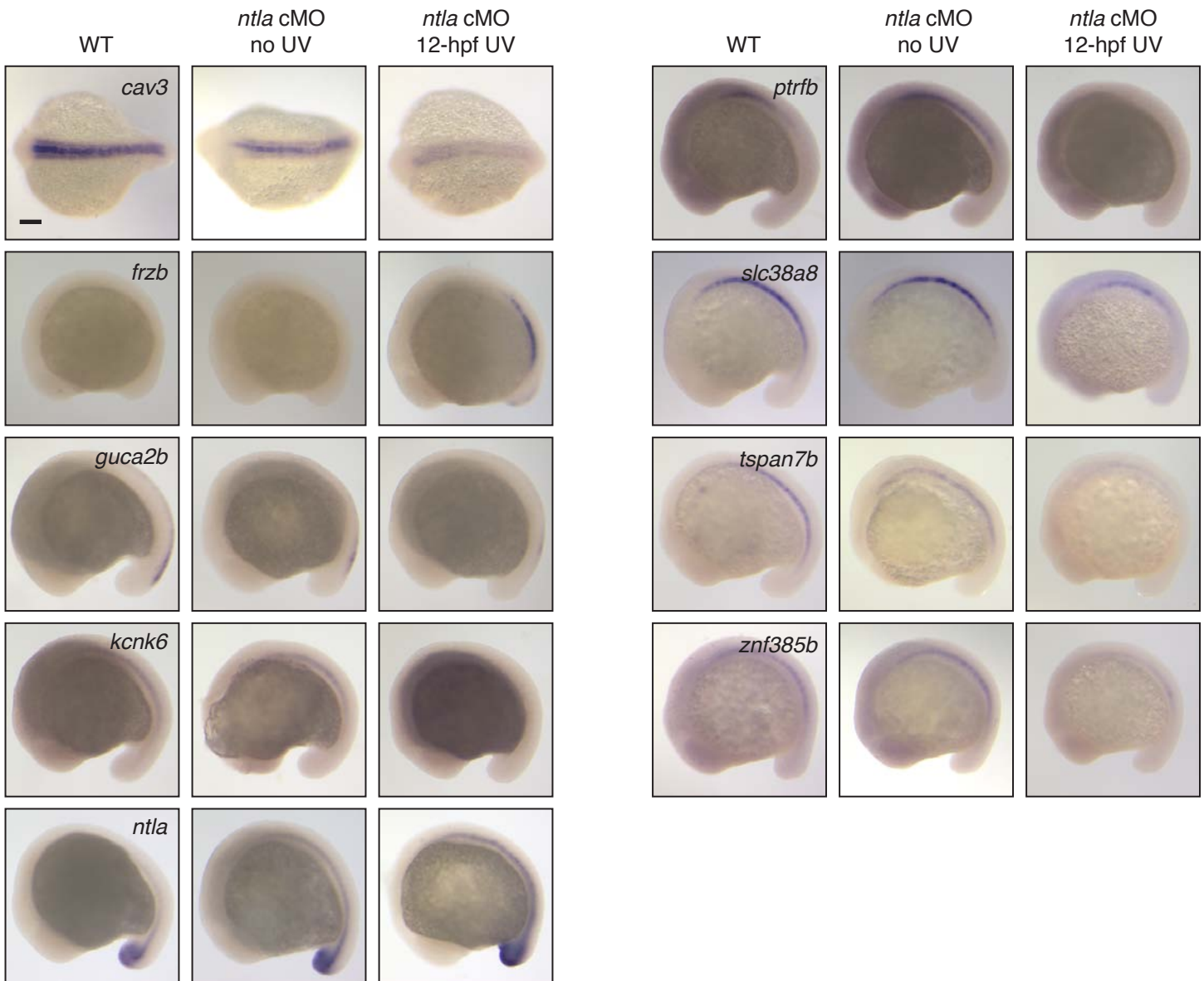


**Supplementary Figure 2. Ntla protein depletion after *ntla* cMO photoactivation within posterior chordamesoderm.**

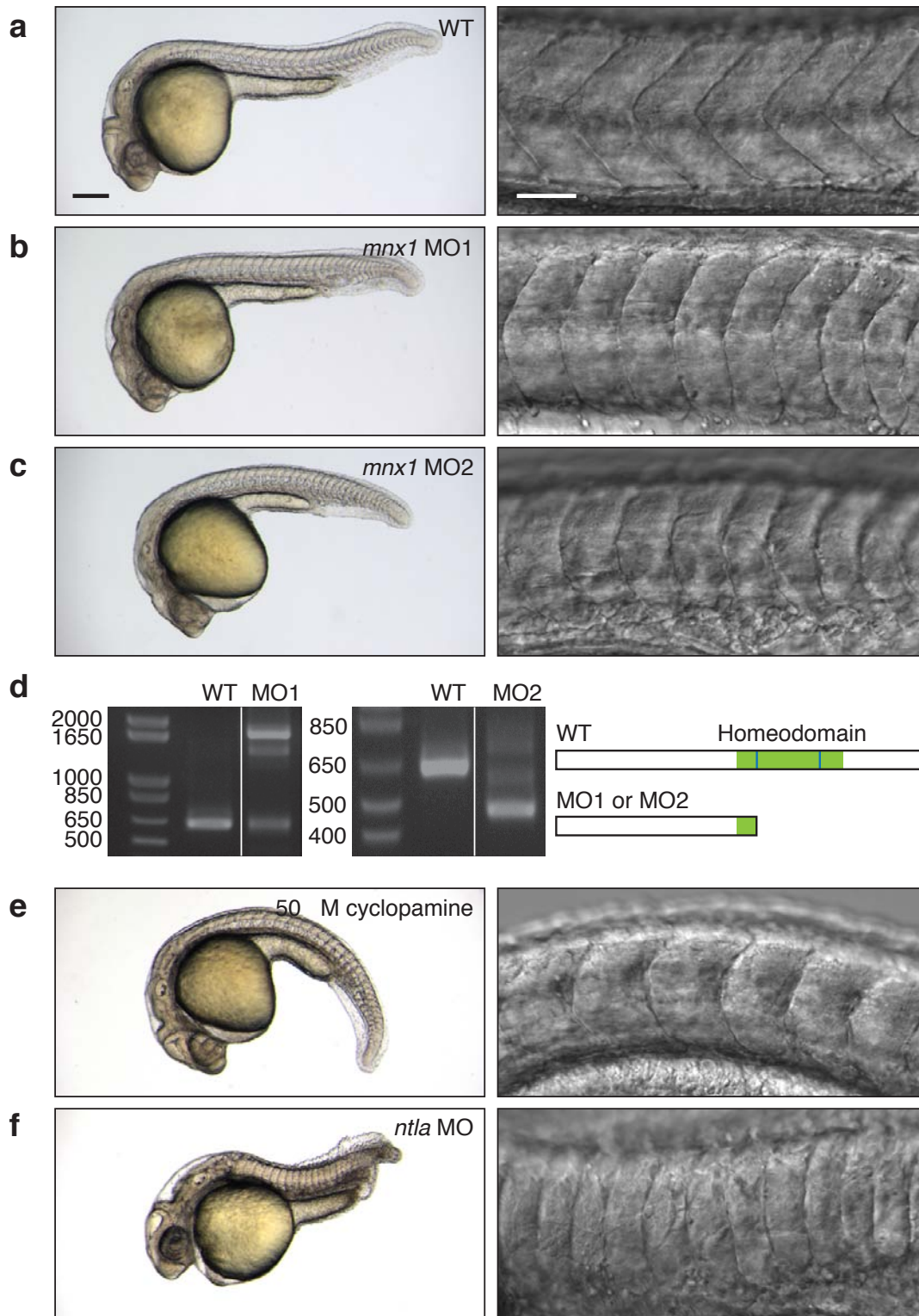
**a**, Zebrafish zygotes were injected with a *ntla* cMO/cFD mixture and then were irradiated within a 100  $\mu$ m-diameter region within the posterior chordamesoderm at 12 hpf. The irradiated embryos were fixed at various time points, and Ntla and FD were detected by immunofluorescence. Non-irradiated embryos were processed and analyzed in an equivalent manner to provide a comparison control, and regions of Ntla protein depletion are indicated by the brackets. **b**, Quantification of Ntla protein levels in 16-hpf embryos after *ntla* cMO photoactivation. Regions demarcated by the dashed white lines were selected for quantification, and image data straightened by ImageJ software is shown below each embryo micrograph. Average pixel intensities for each position along the anterior-posterior axis (arrows) were determined using ImageJ software. Pixel intensities for Ntla immunostaining in non-irradiated (red line) and locally irradiated (dashed red line) embryos are shown, as well as those for FD immunostaining in locally irradiated embryos (green line). Embryo orientations: 12 hpf, dorsal view and anterior up; 14 hpf, posterior dorsal view and dorsal up; 16 hpf, lateral view and anterior left. Scale bars: 200  $\mu$ m.



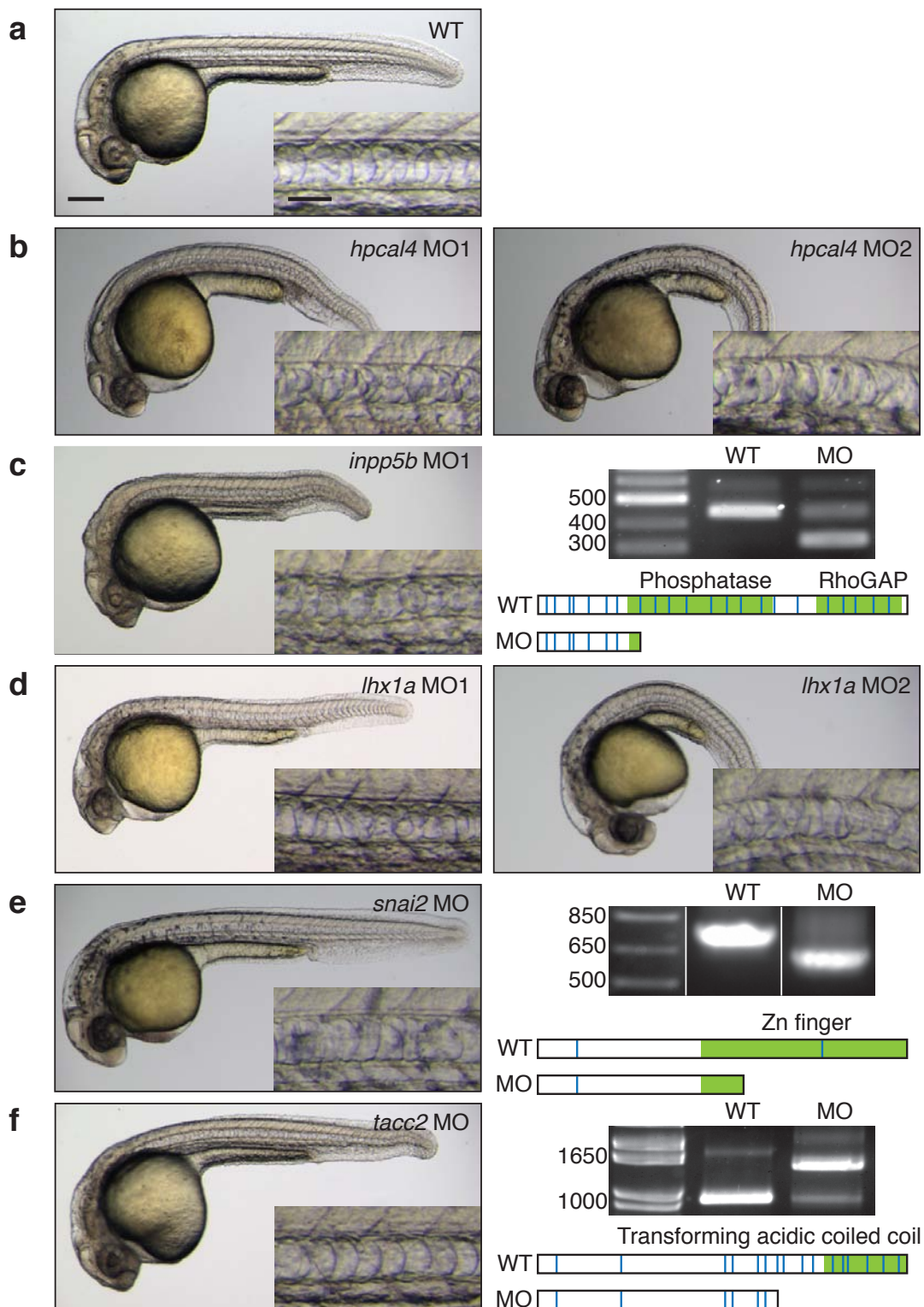
**Supplementary Figure 3. Confirmation of selected microarray hits associated with notochord cell fate commitment by *in situ* hybridization.** 10-hpf wildtype and *ntla* MO-injected embryos stained for candidate Ntla targets expressed during gastrulation are shown, with co-labeling of *pax2a* transcripts in some cases to determine embryo orientation. All 24 genes tested were confirmed to be transcribed in a Ntla-dependent manner. *kirrel3*, *lhx1a*, and *notch1b* transcript levels were specifically reduced in the axial mesoderm of *ntla* morphants, whereas their other expression domains were unaffected. Similarly, expression of *her1*, *rbm38*, *tbx6*, and *wnt8a* in *ntla* morphants was specifically reduced in the tailbud. In addition to these genes, another hit in our microarray data (**Supplementary Table 1**), *wnt3l*, has previously been shown to be expressed in a Ntla-dependent manner (Ref. 4). Embryo orientations: *her1*, *rbm38*, *tbx6*, *wnt8a*, posterior dorsal view and anterior up; all others, dorsal view and anterior up. Scale bar: 100  $\mu$ m.



**Supplementary Figure 4. Confirmation of selected microarray hits associated with notochord maturation by *in situ* hybridization.** 16-hpf *ntlA* cMO-injected embryos that were either cultured in the dark or globally UV irradiated at 12 hpf are shown. Of the nine genes tested, all but *guca2b* were confirmed to be transcribed within the axial mesoderm in a *NtlA*-dependent manner. *cav3* transcript levels were specifically reduced in the chordamesoderm of irradiated embryos, whereas somitic expression was unaffected. The increase in *ntlA* transcript levels upon *ntlA* cMO photoactivation is potentially a consequence of *ntlA* mRNA stabilization by the uncaged MO. Embryo orientations: *cav3*, dorsal view and anterior left; all others, lateral view and anterior left. Scale bar: 100  $\mu$ m.

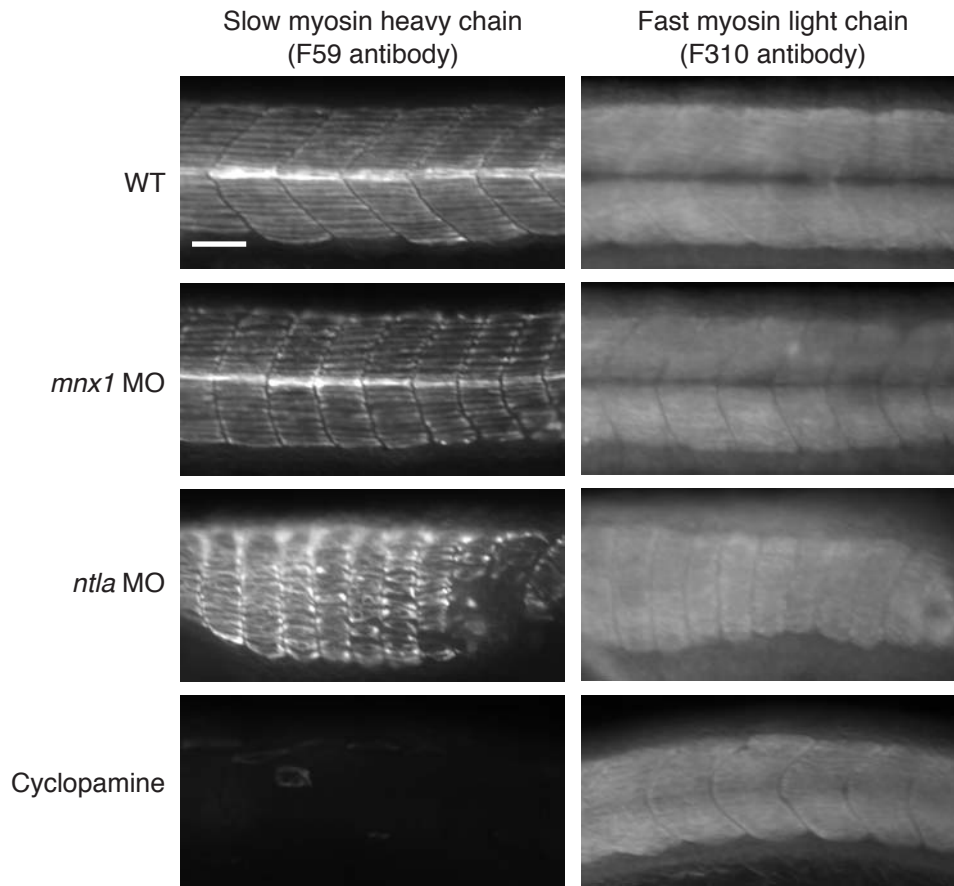


**Supplementary Figure 5. Knockdown of *mnx1* expression induces somite morphology defects that differ from Hedgehog pathway loss-of-function phenotypes.** **a-c**, Somite patterning in wildtype embryos and those previously injected with non-overlapping, splice-blocking *mnx1* MOs. Brightfield and DIC micrographs of 1-dpf embryos are shown. **d**, Confirmation of *mnx1* MO-dependent RNA missplicing by RT-PCR. *Mnx1* proteins encoded by the observed transcripts are shown as bar diagrams, with sites corresponding to exon-intron boundaries depicted as blue lines and known protein domains colored green. Exon-intron assignments are based on the Zv8 zebrafish genome assembly Zv8, gene build 59. **e**, Cyclopamine treatment of embryos starting at 5 hpf resulted in ventral body curvature and U-shaped somites that are shortened along the dorsoventral axis, consistent with loss of Hedgehog pathway-dependent muscle fates. **f**, *ntlA* morphants also exhibited curved somites, but they were morphologically more similar to *mnx1* morphants than to cyclopamine-embryos. Embryo orientations: lateral view and anterior left. Scale bars: whole-embryo brightfield micrograph, 200  $\mu$ m; DIC micrograph, 50  $\mu$ m.

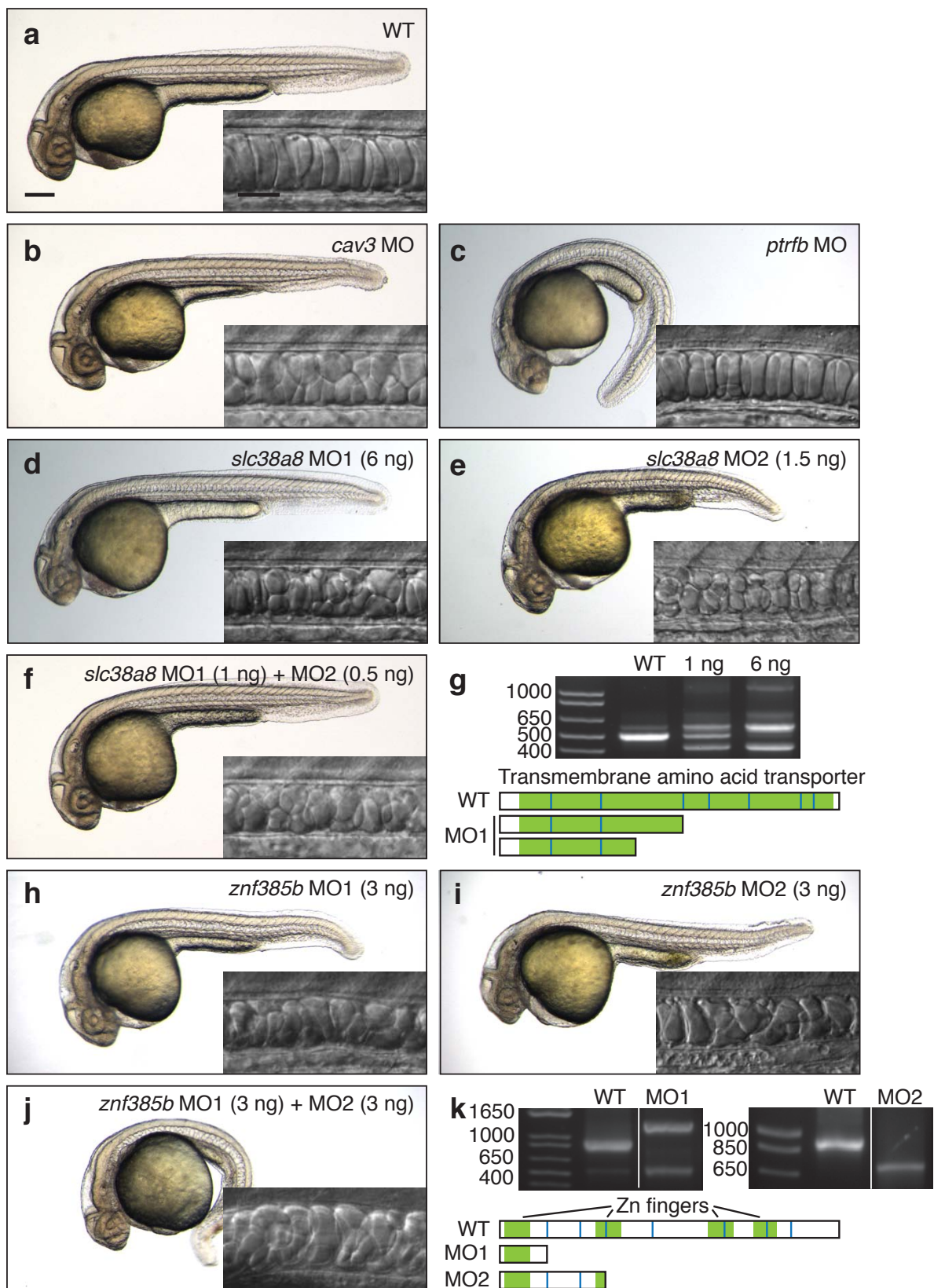


**Supplementary Figure 6. Representative morphants of Ntla-dependent genes expressed during gastrulation that do not exhibit clear notochord defects.** Brightfield micrographs of selected morphants at 1 day post fertilization (dpf) are shown. In cases where a splice-blocking MO was used, RNA missplicing was confirmed by RT-PCR. Proteins encoded by these transcripts are shown as bar diagrams as described in **Supplementary Figure 5**. **a**, Wildtype control. **b**, Embryos injected with two different translation-blocking MOs targeting *hpcal4* at their maximum non-toxic doses exhibited ventral body curvature but wildtype-like notochord cells. **c**, Embryos injected with a splice-blocking MO targeting *inpp5b* had mild notochord necrosis despite co-injection with a *tp53* MO. **d**, Embryos injected with two different translation-blocking MOs targeting *lhx1a* at their maximum non-toxic doses had morphologically normal notochords, although one MO induced ventral curvature and shortening along the anterior-posterior axis. **e-f**, Embryos injected with splice-blocking MOs against *snai2* or *tacc2* had wildtype-like notochords even though the targeted RNA was misspliced as expected. Embryo orientations: lateral view, dorsal up and anterior left. Scale bars: whole-embryo micrograph, 200  $\mu$ m; inset, 50  $\mu$ m.

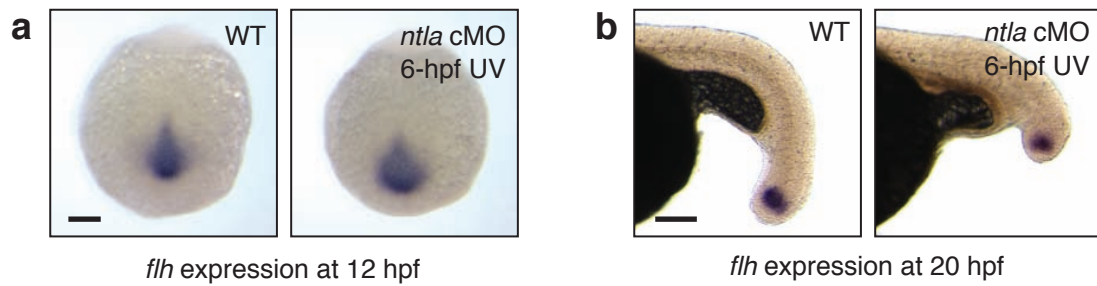




**Supplementary Figure 7. Knockdown of *mnx1* expression induces muscle differentiation defects that differ from Hedgehog pathway loss-of-function phenotypes.** Slow myosin heavy chain and fast myosin light chain expression in wildtype zebrafish and embryos treated with an *mnx1* MO, a *ntla* MO, or 50  $\mu$ M cyclopamine. 1-dpf embryos are shown. Embryo orientations: lateral view and anterior left. Scale bar: 50  $\mu$ m.



**Supplementary Figure 8. Morphants of several Ntla-dependent genes expressed during somitogenesis exhibit aberrant notochord cell morphology.** Brightfield and DIC (inset) micrographs of selected morphants at 1.5 dpf are shown. In cases where a splice-blocking MO was used, RNA missplicing was confirmed by RT-PCR. Proteins encoded by these transcripts are shown as bar diagrams as described in **Supplementary Figure 5**. **a**, Wildtype control. **b**, Embryos injected with a *cav3* MO had disorganized, incompletely vacuolated notochord cells. **c**, Embryos injected with a *ptrfb* MO exhibited reduced notochord cell-cell contacts and ventral body curvature. **d-e**, Embryos injected with either splice-blocking or translation-blocking *slc38a8* MOs (MO1 and MO2, respectively) had incompletely vacuolated notochord cells. **f**, Co-injection of both *slc38a8* MOs at sub-phenotypic doses synergistically induced similar notochord defects. **g**, Confirmation of *slc38a8* MO-dependent RNA missplicing by RT-PCR. **h-i**, Embryos injected with splice-blocking *znf385b* MOs (MO1 or MO2) exhibited partially vacuolated notochord cells. **j**, Co-injection of both *znf385b* MOs led to a stronger notochord defect. **k**, Confirmation of *znf385b* MO-dependent RNA missplicing by RT-PCR. Embryo orientations: lateral view and anterior left. Scale bars: whole-embryo brightfield micrograph, 200  $\mu$ m; DIC inset, 50  $\mu$ m.



**Supplementary Figure 9. Temporal analysis of Ntla-dependent *flh* transcription.** **a-b**, Expression of *flh* at 12 hpf and 20 hpf in wildtype zebrafish, as well as in embryos injected with the *ntla* cMO and irradiated globally at 6 hpf. Embryo orientations: **a**, dorsal posterior view and dorsal up; **b**, lateral view and anterior left. Scale bars: **a**, 100  $\mu$ m; **b**, 200  $\mu$ m.

## SUPPLEMENTARY METHODS

<b>Caged fluorescein dextran</b> .....	37
<b>Ntla polyclonal antibody</b> .....	37-38
<b>Imaging of zebrafish embryos</b> .....	38-39
<b>Cyclopamine treatment of zebrafish embryos</b> .....	39

### **Caged fluorescein dextran (cFD) preparation**

Aminodextran (3.5-5 mg of 10-kDa polymer; Invitrogen, D1860) dissolved in 500  $\mu$ L of 0.1 M  $\text{Na}_2\text{B}_4\text{O}_7$  buffer (pH 8.5) was added to carboxymethylnitrobenzyl (CMNB)-caged fluorescein N-hydroxysuccinimide ester (1 mg; Invitrogen, C20050) in the manufacturer-supplied tinted tube, and the reaction mixture was vortexed overnight. The resulting cFD was separated from unreacted caged fluorescein using a Zeba Desalt spin column (Thermo Fisher Scientific, 89889) according to the manufacturer's instructions. The yellow-colored eluent was lyophilized to dryness, weighed, dissolved in water to make a 1% (w/v) stock solution, and stored at  $-20\text{ }^\circ\text{C}$  as 2- $\mu$ L aliquots. Spectroscopic analysis indicated an average loading of 2.5 caged fluoresceins per dextran molecule.

### **Ntla polyclonal antibody**

Full-length *ntla* cDNA flanked by 5' EcoRI and 3' BamHI sites was generated by PCR using cDNA derived from 10-hpf zebrafish embryos as a template and the following primers: 5'-CGAATTCATGTCTGCCTCAAGTCCCGACCA-3' and 5'-CGGATCCTCAGTAGCTCTGAGCCA-CAGGCG-3'. The *ntla* cDNA was then cloned into a pCR-Blunt II-TOPO vector (Invitrogen), digested with EcoRI and BamHI, and ligated into similarly cut pMALc2x vector (NEB) to generate a bacterial expression construct encoding an Ntla-maltose binding protein (MBP) fusion (pMALc2x-Ntla). The pMALc2X-Ntla vector was transformed into BL21 competent cells and a single colony was cultured in 80 mL LB-ampicillin broth overnight. This starter culture was then used to inoculate 1 L of 2X YT broth (16 g tryptone, 10 g yeast extract, 5 g NaCl, 2 g glucose, 100 mg ampicillin, 1 L water) and cultured for 2 hours at  $37\text{ }^\circ\text{C}$ , followed by 1 hour at  $30\text{ }^\circ\text{C}$  to achieve an  $\text{OD}_{600}$  of 0.8-1.0. IPTG (0.5 mM) was added to the culture, which was grown for another 6 hours at  $30\text{ }^\circ\text{C}$ . Cells were then harvested by centrifugation (4,000  $\times g$ , 20 minutes,  $4\text{ }^\circ\text{C}$ ), resuspended in column buffer (50 mL; 200 mM NaCl, 1 mM EDTA, 0.07% (v/v) 2-mercaptoethanol, 20 mM Tris-HCl, pH 7.4), chilled to  $-72\text{ }^\circ\text{C}$  in a dry ice/ethanol bath,

thawed in ice water, and sonicated 8 x 15 seconds in ice water. Triton X-100 was added to a final concentration of 1% (v/v), and the lysate was mixed gently at 4 °C for 30 minutes to solubilize the Ntla-MBP fusion. The lysate was next centrifuged (12,000 x g, 30 minutes, 4 °C) and the supernatant was passed over amylose resin (5 mL; NEB) that was previously packed into a gravity flow column and equilibrated with the column buffer (40 mL). The loaded amylose resin was washed with column buffer (60 mL) and eluted in 1-mL fractions with column buffer containing 20 mM maltose. Fractions containing the 89 kDa Ntla-MBP fusion protein were pooled and concentrated to 1 mg/mL using an Amicon Centricon centrifugal filter device.

The purified Ntla-MBP fusion protein (4 mg) was cleaved with Factor Xa (40 µg) and Ntla was separated from MBP by DEAE-Sepharose ion exchange chromatography using a pMAL Fusion & Purification System kit (NEB) according to the manufacturer's instructions. Rabbit inoculation and serum collection were conducted by Rockland Immunochemicals using their standard procedures. To affinity purify the polyclonal anti-Ntla antibody, an affinity column was prepared by expressing and purifying the Ntla-MBP fusion protein (4 mg) as described above, dialyzing the protein in 1 L 1X PBS for 12 hours, and immobilizing it onto 1 mL of AminoLink resin (Pierce) according to the manufacturer's instructions. The polyclonal anti-Ntla antibody serum (1 mL) was then passed over the gravity-flow affinity column, eluted with 0.1 M glycine-HCl buffer, pH 2.5-3.0. Each 200-µL fraction containing the purified antibody was then neutralized with 10 µL of 1 M Tris-HCl, pH 9.

### **Imaging of zebrafish embryos**

For live imaging of 24- or 36-hpf zebrafish, the embryos were manually dechorinated and immobilized in E3 medium containing 0.5% (w/v) low-melt agarose and 0.05% (w/v) Tricaine mesylate. Brightfield images were acquired using a Leica M205FA fluorescence stereoscope equipped with a Leica DFC500 digital camera. Differential interference contrast (DIC) micrographs were obtained with a Leica DM4500B epifluorescence microscope equipped

with a 20x/0.5 NA water-immersion objective and a QImaging Retiga-SRV digital camera. Confocal fluorescence and DIC images were obtained with a Zeiss Axio Imager Z1 upright microscope equipped with a 20x/0.5 NA water-immersion objective, fluorescence and transmission photomultiplier tube detectors, and an LSM700 laser-scanning confocal head. Fixed embryos stained by *in situ* hybridization were mounted in 1X PBS containing 2% (w/v) methylcellulose and imaged with the Leica M205FA/DFC500 system using LED illumination arrays and the Leica LAS montage imaging module. Fixed immunostained embryos were mounted in 1X PBS containing 0.5% (w/v) low-melt agarose, and fluorescence images were obtained with a DM4500B/Retiga-SRV system equipped with GFP and TXR filter sets and a 10x/0.30 NA objective.

#### **Cyclopamine treatment of zebrafish embryos**

5-hpf embryos in 10 mL of E3 medium (5 mM NaCl, 0.17 mM KCl, 0.33 mM CaCl<sub>2</sub>, and 0.33 mM MgSO<sub>4</sub>) were treated with an ethanolic solution of cyclopamine (5 µL of a 100 mM stock; 50 µM final concentration) and cultured at 28.5 °C.

## REFERENCES

1. Morley, R.H. et al. A gene regulatory network directed by zebrafish No tail accounts for its roles in mesoderm formation. *Proc. Natl. Acad. Sci. U. S. A.* **106**, 3829-34 (2009).
2. Goering, L.M. et al. An interacting network of T-box genes directs gene expression and fate in the zebrafish mesoderm. *Proc Natl Acad Sci U S A* **100**, 9410-5 (2003).
3. Garnett, A.T. et al. Identification of direct T-box target genes in the developing zebrafish mesoderm. *Development* **136**, 749-60 (2009).
4. Martin, B.L. & Kimelman, D. Regulation of canonical Wnt signaling by Brachyury is essential for posterior mesoderm formation. *Dev. Cell* **15**, 121-33 (2008).
5. Lightcap, C.M. et al. Interaction with LC8 is required for Pak1 nuclear import and is indispensable for zebrafish development. *PLoS One* **4**, e6025 (2009).
6. Lewis, K.E., Bates, J. & Eisen, J.S. Regulation of *iro3* expression in the zebrafish spinal cord. *Dev. Dyn.* **232**, 140-8 (2005).
7. Veeman, M.T., Slusarski, D.C., Kaykas, A., Louie, S.H. & Moon, R.T. Zebrafish *prickle*, a modulator of noncanonical Wnt/Fz signaling, regulates gastrulation movements. *Curr. Biol.* **13**, 680-5 (2003).
8. Gansner, J.M. & Gitlin, J.D. Essential role for the alpha 1 chain of type VIII collagen in zebrafish notochord formation. *Dev. Dyn.* **237**, 3715-26 (2008).
9. Eimon, P.M. et al. Delineation of the cell-extrinsic apoptosis pathway in the zebrafish. *Cell Death Differ.* **13**, 1619-30 (2006).
10. Kottgen, M. et al. TRPP2 and TRPV4 form a polymodal sensory channel complex. *J. Cell Biol.* **182**, 437-47 (2008).
11. Carney, T.J. et al. Genetic analysis of fin development in zebrafish identifies furin and hemicentin1 as potential novel fraser syndrome disease genes. *PLoS Genet.* **6**, e1000907 (2010).



12. van Eeden, F.J. et al. Genetic analysis of fin formation in the zebrafish, *Danio rerio*. *Development* **123**, 255-62 (1996).
13. Harvey, S.A. & Logan, M.P. *sall4* acts downstream of *tbx5* and is required for pectoral fin outgrowth. *Development* **133**, 1165-73 (2006).
14. Luo, T. et al. Inca: a novel p21-activated kinase-associated protein required for cranial neural crest development. *Development* **134**, 1279-89 (2007).
15. Srinivas, B.P., Woo, J., Leong, W.Y. & Roy, S. A conserved molecular pathway mediates myoblast fusion in insects and vertebrates. *Nat. Genet.* **39**, 781-6 (2007).
16. Lorent, K. et al. Inhibition of Jagged-mediated Notch signaling disrupts zebrafish biliary development and generates multi-organ defects compatible with an Alagille syndrome phenocopy. *Development* **131**, 5753-66 (2004).
17. Milan, D.J., Giokas, A.C., Serluca, F.C., Peterson, R.T. & MacRae, C.A. Notch1b and neuregulin are required for specification of central cardiac conduction tissue. *Development* **133**, 1125-32 (2006).
18. Yeo, S.Y., Kim, M., Kim, H.S., Huh, T.L. & Chitnis, A.B. Fluorescent protein expression driven by *her4* regulatory elements reveals the spatiotemporal pattern of Notch signaling in the nervous system of zebrafish embryos. *Dev. Biol.* **301**, 555-67 (2007).
19. Maves, L. et al. Pbx homeodomain proteins direct MyoD activity to promote fast-muscle differentiation. *Development* **134**, 3371-82 (2007).
20. Etard, C. et al. The UCS factor Steif/Unc-45b interacts with the heat shock protein Hsp90a during myofibrillogenesis. *Dev. Biol.* **308**, 133-43 (2007).
21. Chen, Y.H. & Tsai, H.J. Treatment with Myf5-morpholino results in somite patterning and brain formation defects in zebrafish. *Differentiation* **70**, 447-56 (2002).
22. Tan, X., Rotllant, J., Li, H., De Deyne, P. & Du, S.J. SmyD1, a histone methyltransferase, is required for myofibril organization and muscle contraction in zebrafish embryos. *Proc. Natl. Acad. Sci. U. S. A.* **103**, 2713-8 (2006).

23. Seeley, M. et al. Depletion of zebrafish titin reduces cardiac contractility by disrupting the assembly of Z-discs and A-bands. *Circ. Res.* **100**, 238-45 (2007).
24. van Eeden, F.J. et al. Mutations affecting somite formation and patterning in the zebrafish, *Danio rerio*. *Development* **123**, 153-64 (1996).
25. Wingert, R.A. et al. The *cdx* genes and retinoic acid control the positioning and segmentation of the zebrafish pronephros. *PLoS Genet.* **3**, 1922-38 (2007).
26. Alexa, K. et al. Maternal and zygotic *aldh1a2* activity is required for pancreas development in zebrafish. *PLoS One* **4**, e8261 (2009).
27. Bessa, J. et al. *meis1* regulates cyclin D1 and c-myc expression, and controls the proliferation of the multipotent cells in the early developing zebrafish eye. *Development* **135**, 799-803 (2008).
28. Lekven, A.C., Thorpe, C.J., Waxman, J.S. & Moon, R.T. Zebrafish *wnt8* encodes two *wnt8* proteins on a bicistronic transcript and is required for mesoderm and neurectoderm patterning. *Dev. Cell* **1**, 103-14 (2001).
29. Thorpe, C.J., Weidinger, G. & Moon, R.T. Wnt/beta-catenin regulation of the Sp1-related transcription factor *sp5l* promotes tail development in zebrafish. *Development* **132**, 1763-72 (2005).
30. Shimizu, T., Bae, Y.K., Muraoka, O. & Hibi, M. Interaction of Wnt and caudal-related genes in zebrafish posterior body formation. *Dev. Biol.* **279**, 125-41 (2005).
31. Draper, B.W., Stock, D.W. & Kimmel, C.B. Zebrafish *fgf24* functions with *fgf8* to promote posterior mesodermal development. *Development* **130**, 4639-54 (2003).
32. Hanai, J. et al. The muscle-specific ubiquitin ligase atrogenin-1/MAFbx mediates statin-induced muscle toxicity. *J. Clin. Invest.* **117**, 3940-51 (2007).
33. Oates, A.C. & Ho, R.K. Hairy/E(spl)-related (Her) genes are central components of the segmentation oscillator and display redundancy with the Delta/Notch signaling pathway in

- the formation of anterior segmental boundaries in the zebrafish. *Development* **129**, 2929-46 (2002).
34. Hill, M.M. et al. PTRF-Cavin, a conserved cytoplasmic protein required for caveola formation and function. *Cell* **132**, 113-24 (2008).
  35. Nixon, S.J. et al. Zebrafish as a model for caveolin-associated muscle disease; caveolin-3 is required for myofibril organization and muscle cell patterning. *Hum. Mol. Genet.* **14**, 1727-43 (2005).
  36. Ouyang, X. et al. Versatile synthesis and rational design of caged morpholinos. *J. Am. Chem. Soc.* **131**, 13255-69 (2009).
  37. Shestopalov, I.A., Sinha, S. & Chen, J.K. Light-controlled gene silencing in zebrafish embryos. *Nat. Chem. Biol.* **3**, 650-1 (2007).
  38. Robu, M.E. et al. p53 activation by knockdown technologies. *PLoS Genet.* **3**, e78 (2007).